Response to comments

This paper analyzed single particle aerosol mass spectrometer (SPAMS) data for ambient aerosols and found there are relations between CN-/CNO- ion intensities and some other species, such as oxidized organic ions and ammonium. It is an interesting report. But there are some concerns which need to be addressed before publication.

We would like to thank the reviewer for his/her useful comments and recommendations to improve the manuscript. We have addressed the specific comments in the sections below and made the appropriate revisions to the manuscript. Reviewer comments are in black text followed by our response in blue text.

One of the major problems is that this paper attribute oxidized organics to secondary formation. However, it may not be the case. Biomass burning or coal combustion can also produce oxidized organics including large amounts of NOCs. Actually, in many previous single particle mass spectrometry studies, CN- and CNO- were taken as ion markers for combustion sources. The authors need to provide more evidences either to rule out the possibility of primary oxygenated organics and primary NOCs or to distinguish the secondary organics from the primary ones.

Thanks for the suggestion. In our manuscript, oxidized organics, represented as formate at m/z -45 $[HCO_2]^-$, acetate at m/z -59 $[CH_3CO_2]^-$, methylglyoxal at m/z -71 $[C_3H_3O_2]^-$, glyoxylate at m/z -73 $[C_2HO_3]^-$, pyruvate at m/z -87 $[C_3H_3O_3]^-$, malonate at m/z -103 $[C_3H_3O_4]^-$ and succinate at m/z -117 $[C_4H_5O_4]^-$, which are generally regarded as secondary compositions (Zhang et al., 2017; Zauscher et al., 2013; Lee et al., 2003). To make it clear, we revised the original description to "These oxidized organics showed their pronounced diurnal trends with afternoon maximum, and were highly correlated (r = 0.72 - 0.94, p < 0.01) with each other. Therefore, they were primarily attributed to the secondary oxidized organics from photochemical oxidation products of various volatile

organic compounds (VOCs) (Paulot et al., 2011; Zhao et al., 2012; Ho et al., 2011), and the details can be found in our previous publication (Zhang et al., 2019).". Please refer to Lines 136-141 of the revised manuscript.

We strongly agree with the reviewer that biomass burning or coal combustion can also produce oxidized organics and NOCs. As discussed above, these oxidized organics most probably formed from secondary process. In the original manuscript, we provided evidence for the secondary formation of NOCs. However, the primary NOCs cannot be ruled out. In the revised manuscript (line 271-274), we have included the following sentence to mention this: "The unexplained NOCs (~25%) might be linked to the primary emissions, such as biomass burning (Desyaterik et al., 2013). It could be partly supported by the presence of potassium and various carbon ion clusters ($C_n^{+/-}$, n = 1, 2, 3, …) in the mass spectrum of NOCs-containing particles (Fig. 1).".

Another major concern is that how well CN-/CNO- ions can represent total NOCs. Can they represent 25%, 50% or 75% of total NOCs? The paper needs to provide more discussion on this issue.

Thanks for the comment. We understand that it would be better if the exact fraction of NOCs represented by CN^-/CNO^- can be obtained. Unfortunately, how well $[CN]^-$ / $[CNO]^-$ ions could represent NOCs cannot be quantified, although they were the most commonly reported NOCs peaks by single particle mass spectrometry (Silva and Prather, 2000; Zawadowicz et al., 2017; Pagels et al., 2013). In the present study, $[CN]^-$ / $[CNO]^-$ ions are among the major peaks detected by the SPAMS (Fig. 1). A rough estimate from the peak area ratio of $[CN]^-$ / $[CNO]^-$ ions and the most likely NOCs fragments (i.e., various amines, and an entire series of nitrogen-containing cluster ions C_nN^-, n = 1, 2, 3, …) (Silva and Prather, 2000) shows that $[CN]^-$ / $[CNO]^-$ ions may represent more than 90% of these NOCs peaks. It has been added in section 2.2.

Pagels, J., Dutcher, D. D., Stolzenburg, M. R., McMurry, P. H., Galli, M. E., and Gross, D. S.: Fine-particle emissions from solid biofuel combustion studied with single-particle mass spectrometry: Identification of markers for organics, soot, and ash components, J. Geophys. Res.-Atmos., 118, 859-870, doi:10.1029/2012jd018389, 2013.

Silva, P. J., and Prather, K. A.: Interpretation of mass spectra from organic compounds in aerosol time-of-flight mass spectrometry, Anal. Chem., 72, 3553-3562, 2000.

Zawadowicz, M. A., Froyd, K. D., Murphy, D. M., and Cziczo, D. J.: Improved identification of primary biological aerosol particles using single-particle mass spectrometry, Atmos. Chem. Phys., 17, 7193-7212, doi:10.5194/acp-17-7193-2017, 2017.

The third concern is that ammonium sulfate is very difficult to be ionized under 266 nm UV laser. Thus, it is likely that some mass spectra of particles do not contain NH4+ peak but these particles may still contain ammonium sulfate. The authors also need to provide some discussions on this possibility.

Thanks for the comment. It is true that pure ammonium sulfate is very difficult to be ionized under 266 nm UV laser used in our study. In the present study, this may not be the case since we focused on the NOCs-containing particles, in which the Nfs of ammonium varied in a wide range (~40-90%) (Fig. 2). Such possibility has been added in Lines 27-28 of the revised *Supplements*.

Specific comments:

Line 54: how much is "large"? It would be always better to provide a number or range.

Thanks for the comment. We have revised the sentence to "Nitrogen-containing organic compounds (NOCs) substantially contribute to the pool of BrC". And we have also stated that "The particulate organic nitrogen accounts for a large fraction of total airborne nitrogen (~30%)". Please refer to Lines 57-61 of the revised manuscript.

Line 149: "so on" is a bit informal. I would change "so on" to "so forth"

It has been revised as suggested.

Line 220: How do you come up with this statement: ": : :explain over half of the observed variations in NOCs in the atmosphere of Guangzhou."? Please elaborate and provide more details.

Thanks for the comment. Multiple linear regression analysis was performed to predict the RPAs of NOCs generated from oxidized organics and ammonium, showing a close association ($R^2 = 0.71$, $p < 0.01$) between the predicted RPAs and the observed values of NOCs (Fig. 4). Based on this result, we infer that over half of the observed variations of NOCs can be explained by the interactions involving oxidized organics and ammonium. This is also supported by the PMF analysis provided in Fig. 5. The sentence has been revised to "The result indicates that interactions involving oxidized organics and ammonium could explain over half of the observed variations in NOCs in the atmosphere of Guangzhou.", and the discussion can be found in Lines 192-200 of the revised manuscript.

Line 224: Please report if the PMF analysis reaches convergence or not. How much is the error of the PMF modelling in the paper?

Thanks for the comment. Such information has been added in the *Supplements*. It can be found in section "Positive matrix factorization analysis", as "PMF solutions with 2−5 factors were tested and showed convergence results. The relevant Q values and Q_{robust} / Q_{theory} for these solutions are shown in Table S3.", and "An uncertainty of 50% in RPA was used due to the shot-to-shot fluctuations of desorption laser and complex particle matrix (Zauscher et al., 2013)."

Line 387: Check English

Thanks for the comment. We have carefully checked and corrected the syntax errors.

High secondary formation of nitrogen-containing organics (NOCs) and its possible link to oxidized organics and ammonium

Guohua Zhang[1], Xiufeng Lian[1,2], Yuzhen Fu[1,2], Qinhao Lin[1], Lei Li[3], Wei Song[1], Zhanyong Wang[4], Mingjin Tang[1], Duohong Chen[5], Xinhui Bi[1,*], Xinming Wang[1], Guoying Sheng[1]

[1] State Key Laboratory of Organic Geochemistry and Guangdong Key Laboratory of Environmental Resources Utilization and Protection, Guangzhou Institute of Geochemistry, Chinese Academy of Sciences, Guangzhou 510640, PR China

[2] University of Chinese Academy of Sciences, Beijing 100039, PR China

[3] Institute of Mass Spectrometer and Atmospheric Environment, Jinan University, Guangzhou 510632, PR China

[4] School of Intelligent Systems Engineering, Sun Yat-sen University, Shenzhen 518107, PR China

[5] State Environmental Protection Key Laboratory of Regional Air Quality Monitoring, Guangdong Environmental Monitoring Center, Guangzhou 510308, PR China

Correspondence to: Xinhui Bi (bixh@gig.ac.cn)

Highlights

- Nitrogen-containing organics (NOCs) were highly internally mixed with photochemically produced secondary oxidized organics

- ~~More than 50% of~~ NOCs ~~were~~ could be well predicted by ~~secondary formation from~~the variations of these~~-~~ oxidized organics and ammonium

- Higher relative humidity and ~~particle acidity~~NOx may facilitate~~d~~ the ~~formation~~ conversion of these oxidized organics to NOCs

26   **Abstract**

27   Nitrogen-containing organic compounds (NOCs) substantially contribute to light

28   absorbing organic aerosols, although the atmospheric processes responsible for the secondary

29   formation of these compounds are poorly understood. In this study, seasonal atmospheric

30   processing of NOCs were investigated by single particle mass spectrometry in urban

31   Guangzhou from 2013-2014. The relative abundance of NOCs is found to be strongly enhanced

32   ~~by~~ when internal mix~~ing~~ed with the photochemically produced secondary oxidized organics

33   (~~such as~~i.e., formate, acetate, pyruvate, methylglyoxal, glyoxylate, oxalate, malonate and

34   succinate) and ~~. Furthermore, the co-occurrence of NOCs with~~ ammonium ~~was also observed~~.

35   In addition, both the hourly detected particle number and relative abundance of NOCs are

36   highly correlated with those of secondary oxidized organics and ammonium. It is therefore

37   hypothesized that secondary formation of NOCs most likely links to the oxidized organics and

38   ammonium. Results from both multiple linear regression analysis and positive matrix

39   factorization analysis further show that the relative abundance of NOCs could be well predicted

40   ($R^2 > 0.7$, $p < 0.01$) by the oxidized organics and ammonium. Interestingly, the relative

41   abundance of NOCs is inversely correlated with ammonium, ~~while~~ whereas their number

42   fractions are positively correlated. This result suggest~~ss~~ that although the formation of NOCs

43   does require the involvement of NH_3/NH_4^+, the relative amount of ammonium may have a

44   negative effect~~does involvement NH_3/NH_4^-. Multiple linear regression analysis and positive~~

45   ~~matrix factorization analysis were performed to predict the relative abundance of NOCs~~

46   ~~generated from oxidized organics and ammonium.~~The conversion of oxidized organics to

3

47   NOCs is likely facilitated by higher ~~Both results showed close associations ($R^2 > 0.7$, $p < 0.01$)~~

48   ~~between the predicted NOCs and the observed values. Increased~~ humidity and ~~higher particle~~

49   ~~acidity~~NOx ~~may promote the production of NOCs~~. Due to the relatively high ~~contribution of~~

50   oxidized organics and NH_3/NH_4^+, the relative contributions of NOCs in summer and autumn

51   ~~is~~were higher than ~~that~~those in spring and winter. To the best of our knowledge, this is the first

52   direct field observation study reporting a close association between NOCs and both oxidized

53   organics and ammonium. These findings have substantial implications for the role of

54   ammonium in the atmosphere, particularly in models that predict the evolution and deposition

55   of NOCs.

56

57   **Keywords**: nitrogen-containing organic compounds, individual particles, oxidized organics,

58   ammonium, mixing state, single particle mass spectrometry

59

1 Introduction

Organic aerosols that strongly absorb solar radiation are referred to as brown carbon (BrC), capable of a comparable level of light absorption in the spectral range of near-ultraviolet (UV) light as black carbon (Andreae and Gelencser, 2006; Feng et al., 2013; Yan et al., 2018). Nitrogen-containing organic compounds (NOCs) substantially ~~represent a large and complicate fraction of atmospheric aerosols{Nehir, 2018 #21993;Zhang, 2012 #9722;Cape, 2012 #22004}, significantly~~ contribut~~ting~~ting to the pool of BrC (Feng et al., 2013; Mohr et al., 2013; Li et al., 2019), and ~~. Furthermore, NOCs~~ have a major effect on atmospheric chemistry, human health and climate forcing (Noziere et al., 2015; Kanakidou et al., 2005; Shrivastava et al., 2017; De Gouw and Jimenez, 2009). The particulate organic nitrogen ~~component of NOCs~~ accounts for a large fraction of total airborne nitrogen (~30%), although the proportion exhibits a high variability temporally and spatially, and therefore has an influence on both regional and global N deposition (Neff et al., 2002; Shi et al., 2010; Cape et al., 2011). However, the sources, evolution and optical properties of NOCs remain unclear and contribute significantly to uncertainties in the estimation of their impacts on the environment and climate (Laskin et al., 2015; Feng et al., 2013).

NOCs are ubiquitous components of atmospheric aerosols, cloud water and rainwater (Altieri et al., 2009; Desyaterik et al., 2013; Laskin et al., 2015), spanning a wide range of molecular weights, structures and light absorption properties (Lin et al., 2016). Emissions of primary NOCs have been attributed to biomass burning, coal combustion, vehicle emissions,

80   biogenic production and soil dust (Laskin et al., 2009; Desyaterik et al., 2013; Sun et al.,

81   2017; Mace et al., 2003; Rastogi et al., 2011; Wang et al., 2017). A Ggrowing body of

82   evidence from laboratory studies suggests that secondary NOCs may be produced in gas

83   phase, aerosol, and clouds. Maillard reactions involving mixtures of atmospheric aldehydes

84   (e.g., methylglyoxal/glyoxal) and ammonium/amines are of particular interests (e.g.,

85   Hawkins et al., 2016; De Haan et al., 2017; De Haan et al., 2011). Similarly, aA significant

86   portion of NOCs may also be derived from the heterogeneous ageing of secondary organic

87   aerosol (SOA) with NH_3 / NH_4^+ (Liu et al., 2015; Laskin et al., 2015). Mang et al. (2008)

88   proposed that even trace levels of ammonia may be sufficient to form NOCs via this pathway.

89   In addition, gas phase formation of NOCs through interaction between volatile organic

90   hydrocarbons and NO_x and other oxidations, followed by condensation may also have

91   potential contribution (Fry et al., 2014; Stefenelli et al., 2019; Lehtipalo et al., 2018).

92   The secondary formation of NOCs is especially prevalent in environments experiencing

93   high anthropogenic emissions (Yu et al., 2017; Ho et al., 2015), although further studies are

94   required to comprehensively establish the formation mechanisms. A major obstacle is that

95   organic and inorganic matrix effects have a profound impact on the chemistry of organic

96   compounds in bulk aqueous particles and particles undergoing drying (El-Sayed et al., 2015;

97   Lee et al., 2013). While real-time characterization studies remain a challenge due to the

98   extremely complex chemical nature of NOCs, establishing this data along with the co-

99   variation of NOCs with other chemical components would help to identify the sources and

100   evolution of NOCs. Using single-particle aerosol time-of-flight mass spectrometry, Wang et

6

101 al. (2010) observed that the widespread occurrence of NOCs was closely correlated with

102 particle acidity in the atmosphere of Shanghai (China). In addition, real-time measurements

103 of the atmosphere in New York (US) by aerosol mass spectrometry, indicated a positive link

104 between the age of organic species and the N/C ratio (Sun et al., 2011). Further in-depth

105 studies are required to identify the role of formation conditions (e.g., relative humidity (RH)

106 and pH) for secondary NOCs (Aiona et al., 2017; Nguyen et al., 2012). In present study, the

107 mixing state of individual particles were investigated, involving NOCs, oxidized organics

108 and ammonium, based on on-line seasonal observations using a single particle aerosol mass

109 spectrometry (SPAMS). Our findings show that the formation of NOCs is significantly

110 linked to oxidized organics and NH_4^+, which has important environmental implications for

111 assessing the impact and fate of these compounds.

112

113 **2 Methods**

114 **2.1 Field measurements**

115   Sampling was performed at the Guangzhou Institute of Geochemistry, a representative

116 urban site in Guangzhou (China), a megacity in the Pearl River Delta (PRD) region. SPAMS

117 analysis was performed (Hexin Analytical Instrument Co., Ltd., China) to establish the size

118 and chemical composition of individual particles in real-time (Li et al., 2011). The sampling

119 inlet for aerosol characterization was situated 40 meters above the ground level. A brief

120 description of the performance of SPAMS and other instruments can be found in the

121 Supporting Information. The sampling periods covered four seasons including spring (21/02

122 to 11/04 2014), summer (13/06 to 16/07 2013), autumn (26/09 to 19/10 2013) and winter

123 (15/12 to 25/12 2013). The total measured particle numbers and mean values for

124 meteorological data and gaseous pollutants, are outlined for each season in Table S1 and

125 were described in a previous publication (Zhang et al., 2019).

126

127 **2.2 SPAMS data analysis**

128   Fragments of NOCs were identified according to detection of ion peaks at m/z -26 $[CN]^-$

129 or -42 $[CNO]^-$, generally due to the presence of C-N bonds (Silva and Prather, 2000;

130 Zawadowicz et al., 2017; Pagels et al., 2013). Laboratory produced C-N bonds compounds

131 from bulk solution-phase reactions between the representative oxidized organics (i.e.,

132 methylglyoxal) and ammonium sulfate was used to confirm the generation of ion peaks at

133 m/z -26 $[CN]^-$ and/or -42 $[CNO]^-$ using SPAMS (Fig. S1). Thus, the NOCs herein may refer

134 to complex nitrated organics such as organic nitrates, nitro-aromatics, nitrogen heterocycles

135 and polyphenols. Unfortunately, how well $[CN]^-$/ $[CNO]^-$ ions could represent NOCs cannot

136 be quantified, although they were the most commonly reported NOCs peaks by single

137 particle mass spectrometry (Silva and Prather, 2000; Zawadowicz et al., 2017; Pagels et al.,

138 2013). In the present study, $[CN]^-$/ $[CNO]^-$ ions are among the major peaks detected by the

139 SPAMS (Fig. 1). A rough estimate from the peak area ratio of $[CN]^-$/ $[CNO]^-$ ions and the

140 most likely NOCs fragments (i.e., various amines, and an entire series of nitrogen-containing

141 cluster ions C_nN^-, n = 1, 2, 3, …) (Silva and Prather, 2000) shows that $[CN]^-$/ $[CNO]^-$ ions

142 may represent more than 90% of these NOCs peaks. The number fractions (Nfs) of particles

143   that contained NOCs ranged from 56-59% across all four seasons (Table S1). The number

144   of detected NOCs-containing particles distributing along their vacuum aerodynamic

145   diameter (d_{va}) is shown in Fig. S2. Most of the detected NOC-containing particles had a d_{va}

146   in a range of 300-1200 nm.

147   A representative mass spectrum for NOCs-containing particles is shown in Fig. 1.

148   Dominant peaks in the mass spectrum were 39 [K]$^+$, 23 [Na]$^+$, nitrate (-62 [NO$_3$]$^-$ or -46

149   [NO$_2$]$^-$), sulfate (-97 [HSO$_4$]$^-$), organics (27 [C$_2$H$_3$]$^+$, 63 [C$_5$H$_3$]$^+$, -42 [CNO]$^-$, -26 [CN]$^-$),

150   ammonium (18 [NH$_4$]$^+$) and carbon ion clusters (C$_n^{+/-}$, n = 1, 2, 3,…). NOCs-containing

151   particles were internally mixed with various oxidized organics, represented as formate at m/z

152   -45 [HCO$_2$]$^-$, acetate at m/z -59 [CH$_3$CO$_2$]$^-$, methylglyoxal at m/z -71 [C$_3$H$_3$O$_2$]$^-$, glyoxylate

153   at m/z -73 [C$_2$HO$_3$]$^-$, pyruvate at m/z -87 [C$_3$H$_3$O$_3$]$^-$, malonate at m/z -103 [C$_3$H$_3$O$_4$]$^-$ and

154   succinate at m/z -117 [C$_4$H$_5$O$_4$]$^-$ (Zhang et al., 2017; Zauscher et al., 2013; Lee et al., 2003).

155   These oxidized organics showed their pronounced diurnal trends with afternoon maximum,

156   and were highly correlated (r = 0.72 - 0.94, p < 0.01) with each other. Therefore, they were

157   primarily attributed to The contribution of these ion peaks to the formation of secondary

158   oxidized organics from photochemical oxidation products of various volatile organic

159   compounds (VOCs) (Paulot et al., 2011; Zhao et al., 2012; Ho et al., 2011), and the details

160   can be found in our previous publication has been previously confirmed based on their

161   pronounced diurnal trends, with maximum concentrations observed in the afternoon (Zhang

162   et al., 2019). Furthermore, these oxidized organics have been reported to be highly correlated

163   (r = 0.72 - 0.94, p < 0.01) with each other (Zhang et al., 2019), consistent with the assumption

164 ~~that they are photochemical oxidation products of various volatile organic compounds~~

165 ~~(VOCs) (Paulot et al., 2011; Zhao et al., 2012; Ho et al., 2011).~~ More information on the

166 seasonal variation range of the Nfs of oxidized organics, ammonium and NOCs is presented

167 in Fig. S3.

168   Hourly mean Nfs and relative peak areas were applied herein to indicate the variations

169 of aerosol compositions in individual particles. Even though advances have been made in

170 the quantification of specific chemical species for individual particles based on their

171 respective peak area information, it is still quite a challenge for SPAMS to provide

172 quantitative information on aerosol components mainly due to matrix effects, incomplete

173 ionization and so forth (Qin et al., 2006; Jeong et al., 2011; Healy et al., 2013; Zhou et al.,

174 2016). Despite of this, the variation of relative peak area should be a good indicator for the

175 investigation of atmospheric processing of various species in individual particles (Wang et

176 al., 2010; Zauscher et al., 2013; Sullivan and Prather, 2007; Zhang et al., 2014).

177

178 **3 Results and Discussion**

179 **3.1 Evidence for the formation of NOCs from oxidized organics and ammonium**

180   Figure 2 shows the seasonal variations in Nfs of the oxidized organics and ammonium,

181 which were internally mixed with NOCs. On average, more than 90% of the oxidized

182 organics and 65% of ammonium (except spring) were found to be internally mixed with

183 NOCs (Fig. S4). Regarding that ~~Based on the comparison of~~ the Nfs of NOCs ~~(~60%)~~

184 relative to all the measured particles was ~60%, it could be concluded that NOCs were

185 enhanced with the presence of oxidized organics and ammonium, with the enhancement

186 associated with oxidized organics being the most pronounced.

187   A strong correlation between both the Nfs and relative peak areas (RPAs) of NOCs and

188 oxidized organics further demonstrates a their close associations between these factors, as

189 shown in Fig. 3. Compared with the variation in oxidized organics, the Nfs of ammonium-

190 containing particles internally mixed with NOCs varied within a wider range (~40-90%).

191 However, there was is still an enhancement mixing of NOCs with ammonium. In addition,

192 aA positive correlation ($R^2 = 0.50$, $p < 0.01$) is observed between the hourly detected number

193 of NOCs and ammonium. In contrast, It is worth noting that a negative correlation ($R^2 = 0.55$,

194 $p < 0.01$) is obtained between the hourly average RPAs of NOCs and ammonium (Fig. 3).

195 Interestingly, the relationship between NOCs and ammonium was distinctly different from

196 the relationship between NOCs and oxidized organics. A positive correlation ($R^2 = 0.50$, p

197 < 0.01) was observed between the hourly detected number of NOCs and ammonium. In

198 contrast, a negative correlation ($R^2 = 0.55$, $p < 0.01$) was observed between the hourly

199 average relative peak areas (RPAs) of NOCs and ammonium (Fig. 3).

200   Based on both the enhancement of NOCs and the high correlations with oxidized

201 organics and ammonium, it is hypothesized that interactions between oxidized organics and

202 ammonium contributed to the observed NOCsthe dominant association between oxidized

203 organics and NOCs (Fig. 2) indicates that NOCs may be formed from the processing of

204 secondary oxidized organics in particle phase, rather than gas phase reactions followed by

205 condensation. Actually, formation of NOCs from ammonium and carbonyls has been

confirmed in several laboratory studies (Sareen et al., 2010; Shapiro et al., 2009; Noziere et al., 2009; Kampf et al., 2016; Galloway et al., 2009). Secondary organic aerosols (SOA) produced from a large group of biogenic and anthropogenic VOCs can be further aged by NH_3/NH_4^+ to generate NOCs (Nguyen et al., 2012; Bones et al., 2010; Updyke et al., 2012; Liu et al., 2015; Huang et al., 2017). In a chamber study, the formation of NOCs were found to beis enhanced in a NH_3-rich environment (Chu et al., 2016). While such chemical mechanisms might be complex, the initial steps generally involve reactions forming imines and amines, which can further react with carbonyl SOA compounds to form more complex products (e.g., oligomers/BrC) (Laskin et al., 2015).

To verify this hypothesis, multiple linear regression analysis was is performed to test how well could the RPAs of NOCs could be predicted by the oxidized organics and ammonium. As expected, there is a close association ($R^2 = 0.71$, $p < 0.01$) between the predicted RPAs and the observed values of NOCs (Fig. 4), which supports this hypothesis. An obvious substantial improvement in R^2 implies that a model that uses both oxidized organics and ammonium to predict RPAs of NOCs is substantially better than one that uses only one predictor (either oxidized organics or ammonium in Fig. 3). The result indicates that interactions involving oxidized organics and ammonium could explain over half of the observed variations in NOCs in the atmosphere of Guangzhou. A fraction of the unaccounted NOCs could be due to primary emissions and other formation pathways.

Actually, formation of NOCs from ammonium and carbonyls have been confirmed in several laboratory studies (Sareen et al., 2010; Shapiro et al., 2009; Noziere et al., 2009;

227 ~~Kampf et al., 2016; Galloway et al., 2009). Secondary organic aerosols (SOA) produced~~

228 ~~from a large group of biogenic and anthropogenic VOCs can be further aged by NH_3/NH_4^+~~

229 ~~to generate NOCs (Nguyen et al., 2012; Bones et al., 2010; Updyke et al., 2012; Liu et al.,~~

〔域代码已更改〕

230 ~~2015; Huang et al., 2017). In a chamber study, the formation of NOCs were found to be~~

231 ~~enhanced in a NH_3-rich environment (Chu et al., 2016). While such chemical mechanisms~~

232 ~~might be complex, the initial steps generally involve reactions forming imines and amines,~~

233 ~~which can further react with carbonyl SOA compounds to form more complex products (e.g.,~~

234 ~~oligomers/BrC) (Laskin et al., 2015).~~

〔域代码已更改〕

235

236

237 Th~~is~~e hypothesis could also be supported by the similar pattern of diurnal variation

238 observed for NOCs and oxidized organics (Fig. S5), although there is a slight lag ~~period was~~

239 ~~observed in~~for the ~~the overnight peaks of~~ NOCs. Such diurnal pattern is similar to those

240 observed in Beijing and Uintah (Yuan et al., 2016; Zhang et al., 2015). Notably, such diurnal

241 pattern of secondary NOCs is effectively modelled when the production of NOCs via

242 carbonyls and ammonium is included (Woo et al., 2013). I~~n addition to~~ possible photo-

243 bleaching (Zhao et al., 2015), t~~he lower contribution of NOCs during daytime may be partly~~

244 explained by the lower RH, as discussed in section 3.2.

245 Interestingly, the relationship between NOCs and ammonium is distinctly different

246 from the relationship between NOCs and oxidized organics (Fig. 3). ~~Water soluble organic~~

247 ~~nitrogen (WSON) was reported to be positively correlated with some oxidation products in~~

a forest in northern Japan (Miyazaki et al., 2014). This is further supported by the similar pattern of diurnal variation observed for NOCs and oxidized organics (Fig. S6). However, a slight lag period was observed in the overnight peaks of NOCs, as compared to those of the oxidized organics. This finding was consistent with previously reported results, showing NOCs to have concentration maxima overnight in Beijing and Uintah (Yuan et al., 2016; Zhang et al., 2015). The lower contribution of NOCs during daytime may be partly explained by the lower RH, as discussed in section 3.2, in addition to photo-bleaching which occurs during daytime (Zhao et al., 2015).

Interestingly, the relationship between NOCs and ammonium was distinctly different from the relationship between NOCs and oxidized organics. A positive correlation ($R^2 = 0.50$, $p < 0.01$) was observed between the hourly detected number of NOCs and ammonium. In contrast, a negative correlation ($R^2 = 0.55$, $p < 0.01$) was observed between the hourly average relative peak areas (RPAs) of NOCs and ammonium (Fig. 3). This implies that the controlling factors on the formation of NOCs from ammonium are different from those controlling oxidized organics. On one hand, the positive correlation between the detected numbers reflects that the formation of NOCs does require the participant of NH_3/NH_4^+, consistent with the enhancement of NOCs in ammonium-containing particles discussed above. On the other hand, the negative correlation between the RPAs signifies that particles with higher relative ammonium content may inhibit the formation of NOCs. the relative amount of ammonium may influences the formation of NOCs. Consistently, there is a negative correlation between concentrations of WSON and NH_4^+ in filter samples (Fig. S6).

269   This is supported by the inverse correlation between that Nfs of ammonium that internally

270   mixed with NOCs and the RPAs of ammonium (Fig. S7). This is also theoretically possible

271   since the formation of NOCs may be influenced by particle acidity (Miyazaki et al., 2014;

272   Aiona et al., 2017; Nguyen et al., 2012), which is substantially affected by the abundance of

273   ammonium. Particle acidity could also play a significant role in the gas-to-particle

274   partitioning of aldehydes (Herrmann et al., 2015; Liggio et al., 2005; Gen et al., 2018; De

275   Haan et al., 2018; Kroll et al., 2005), precursors for the formation of oxidized organics.

276   Consistently, higher relative acidity was observed for the internally mixed ammonium and

277   NOCs particles, compared to ammonium-containing particles without NOCs (Fig. S6), and

278   thus may influence the formation of NOCs (Fig. S7). However, the higher relative acidity

279   might also be a result of NOCs formation. A model simulation shows that after including the

280   chemistry of SOA ageing with NH_3, an increase in aerosol acidity would be expected due to

281   the reduction in ammonium (Zhu et al., 2018). It is also noted that the particle acidity is

282   roughly estimated by the relative abundance of ammonium, nitrate, and sulfate in individual

283   particles (Denkenberger et al., 2007), and thus may not be representative of actual aerosol

284   acidity or pH (Guo et al., 2015; Hennigan et al., 2015; Murphy et al., 2017). In addition,

285   ammonia in gas phase is also efficient at producing NOCs (Nguyen et al., 2012), which may

286   play a complex role in the distribution of ammonium and NOCs in particulate phase. The

287   formation of ammonium and NOCs would compete for ammonia, which may also potentially

288   result in the negative correlation between the RPAs of NOCs and ammonium. Unfortunately,

289   such a role remains unclear since the variations of ammonia were not available in the present

290 study. This finding was consistent with the results discussed in section 3.1, indicating that

291 particles containing a higher abundance of ammonium may not facilitate the formation of

292 NOCs.

293 Similarly, ambient observations reported from a forest site in Japan indicate that aerosol

294 acidity likely plays an important role in the formation of WSON via acid-catalyzed reactions

295 in summer (Miyazaki et al., 2014). Enhanced organic aerosol yields from gas-phase

296 carbonyls in the acidic seed aerosol have been attributed to the occurrence of acid-catalyzed

297 reactions (Jang et al., 2002). Furthermore, acidity could also play a significant role in the

298 gas to particle partitioning of aldehydes (Herrmann et al., 2015; Liggio et al., 2005; Gen et

299 al., 2018; De Haan et al., 2018; Kroll et al., 2005), although some studies have indicated that

300 browning of some SOA occurs independently within a pH range of 4−10 (Nguyen et al.,

301 2012). Consistently higher relative acidity was observed for the internally mixed ammonium

302 and NOCs particles, as compared to ammonium containing particles without NOCs (Fig.

303 S7). This may be due to the fact that the ammonium available to react with secondary

304 oxidized organics was from the uptake of ammonia, regarding that NOCs were mainly

305 supplied by heterogeneous reactions of oxidized organics, as discussed above. In this case,

306 the formation of ammonium and NOCs would compete for ammonia, potentially resulting

307 in a negative correlation between the RPAs of NOCs and ammonium as observed (Fig. 3).

308 A study shows that ammonia is more efficient at producing NOC than ammonium (Nguyen

309 et al., 2012). The negative correlation between concentrations of WSON and NH_4^- in filter

310 samples (Fig. S7), may serve as quantitative support for the close association between

311 WSON formation and NH_4^+. Furthermore, the negative correlation between the RPA of

312 NOCs and ammonium, may indicate that the formation of NOCs is influenced by particle

313 acidity, Consistently, the Nfs of ammonium that internally mixed with NOCs were inversely

314 correlated with the RPAs of ammonium (Fig. S8). {Guo, 2015 #22779;Hennigan, 2015

315 #22780;Murphy, 2017 #22781}which is directly affected by the abundance of ammonium

316 (as discussed in section 3.3). Consistently, the Nfs of ammonium that internally mixed with

317 NOCs were inversely correlated with the RPAs of ammonium (Fig. S8).

318 One may expect that NOCs were formed through the interactions between NOx and

319 oxidized organics in gas phase followed by condensation (Fry et al., 2014; Stefenelli et al.,

320 2019; Lehtipalo et al., 2018). However, low correlation coefficients (R^2 = 0.02-0.13)

321 between NOCs and NOx indicates limited contribution of this pathways to the observed

322 NOCs. Also, NOCs formed through NOx and oxidized organics followed by partitioning

323 would not be dependent on the amount of ammonium, which is incompatible with our results.

324 Multiple linear regression analysis was performed to predict the RPAs of NOCs

325 generated from oxidized organics and ammonium, showing a close association (R^2 = 0.71,

326 $p < 0.01$) between the predicted RPAs and the observed values of NOCs (Fig. 4). Therefore,

327 the interactions involving oxidized organics and ammonium may explain over half of the

328 observed variations in NOCs in the atmosphere of Guangzhou. A fraction of the unaccounted

329 NOCs could be due to primary emissions and other formation pathways.

330 **3.2 Factors contributing to the NOCs resolved by positive matrix factorization (PMF)**

331 **analysis**

332 ~~Consistent results were also obtained from the PMF model analysis (Norris et al., 2009)~~

333 ~~(detailed information is provided in the SI).~~ Fig<u>ure</u>~~.~~ 5 presents the PMF factor profiles

334 <u>obtained from the PMF model analysis (detailed information is provided in the SI) (Norris</u>

335 <u>et al., 2009)</u> and their diurnal variations. Around 75% of NOCs could be well explained by

336 two factors, with 33% of the ~~modelled~~<u>PMF resolved</u> NOCs mainly associated with

337 ammonium and carbonaceous ion peaks (ammonium factor), while 59% were mainly

338 associated with oxidized organics (oxidized organics factor). <u>The explained fraction of</u>

339 <u>NOCs by the ammonium and oxidized organic factors is consistent with the linear regression</u>

340 <u>analysis. In addition, PMF analysis provided information on the factor contribution and</u>

341 <u>diurnal variations, which may help explain the seasonal variations and processes of NOCs.</u>

342 The ammonium factor showed a diurnal variation pattern peaking during early morning,

343 which is consistent with the diurnal variation in RH (Zhang et al., 2019). ~~In addition, t~~<u>T</u>his

344 factor contributed to ~80% (Fig. S8) of the <u>PMF resolved</u> ~~modelled~~ NOCs during spring

345 <u>with</u> ~~when~~ the highest RH ~~was observed~~ (Table S1)<u>, whereas</u> ~~, while~~ the oxidized organics

346 factor dominated <u>(> 80%)</u> in ~~all~~ <u>summer and fall</u>~~other seasons~~. <u>In winter, these two factors</u>

347 <u>similarly contributed (~40%). This may indicate a potential role of aqueous pathways in the</u>

348 <u>formation of NOCs, particularly during spring.</u> Differently, the oxidized organics factor

349 showed a pattern of diurnal variation, increasing from morning hours and peaking overnight,

350 which may correspond to the photochemical production of oxidized organics and follow-

351 ~~up~~<u>ed</u> interaction<u>s</u> with condensed ammonium. This pathway may explain the slightly late

352 peaking of NOCs compared to oxidized organics, as ~~condensation of~~ ammonium

18

353 condensation is favorable overnight (Hu et al., 2008). While there were similarities in the

354 fractions of oxidized organics in the oxalate factor and the oxidized organics factor, they

355 only contributed to 8% of the PMF resolved modelled NOCs in the oxalate factor, which

356 contained ~80% of the PMF resolvedmodelled oxalate. As previously discussed, these

357 oxidized organics are also precursors for the formation of oxalate (Zhang et al., 2019).

358 Therefore, the PMF results and therefore, these results suggest that there were are two

359 competitive pathways for the evolution of these oxidized organics. Some oxidized organics

360 formed from photochemical activities were further oxidized to oxalate, resulteding in a

361 diurnal pattern of variation and with concentration peaks during the afternoon (Fig. 5), while

362 others interact with NH_3/NH_4^+ ammonium to form NOCs, peaking during the nighttime.

363 However, the controlling factors for these pathways could not be determined in the present

364 study. The unexplained NOCs (~25%) might be linked to the primary emissions, such as

365 biomass burning (Desyaterik et al., 2013). It could be partly supported by the presence of

366 potassium and various carbon ion clusters ($C_n^{+/-}$, n = 1, 2, 3, …) in the mass spectrum of

367 NOCs-containing particles (Fig. 1).

368

369

370 **3.2 3 Seasonal variations in the observed NOCs**

371   There is aA clear seasonal variation in of NOCs were also observed, with higher relative

372 contributions during summer and autumn (Figs. 3 and 4), mainly due to the variations in

373 oxidized organics and NH_3/NH_4^+. As discussed in section 3.3, particle acidity was lower

19

374 ~~during spring and winter than during summer and autumn, which may contribute to the~~

375 ~~observed seasonal variations.~~ In this region, a larger contribution from secondary oxidized

376 organics is typically observed during summer and autumn (Zhou et al., 2014; Yuan et al.,

377 2018). The seasonal maximum NH_3 concentrations have also been reported during the

378 warmer seasons, corresponding to the peak emissions from agricultural activities and high

379 temperatures, while the low NH_3 concentrations observed in colder seasons may be

380 attributed to gas-to-particle conversion (Pan et al., 2018; Zheng et al., 2012). Such seasonal

381 variation in NOCs ~~were~~ is also obtained in a model simulation, showing that the conversion

382 of NH_3 into NOCs would result in a significantly higher reduction of gas-phase NH_3 during

383 summer (67%) than winter (31%), due to the higher NH_3 and SOA concentrations present

384 in the summer (Zhu et al., 2018). More primary NOCs may also be present during summer

385 and autumn in the present study, due to the additional biomass burning activities in these

386 seasons (Chen et al., 2018; Zhang et al., 2013).

387 ~~While t~~The seasonal variations ~~in~~ of NOCs can be adequately explained by the

388 variations in concentrations of oxidized organics and ammonium (Fig. 4), although the

389 hourly variations during each season ~~were~~ are not well explained, as indicated by the lower

390 R^2 values (Table S2). The correlation coefficients (R^2) range~~d~~ from 0.24 to 0.57 for inter-

391 seasonal variations~~, although all~~ the regressions were found to be significant. ~~As shown in~~

392 ~~Fig. 3, the seasonal dependence~~variation of NOCs ~~on oxidized organics and ammonium~~

393 ~~varies~~was dependent on seasons, despite the correlations between NOCs and oxidized

394 ~~organics / ammonium being significant (*p* < 0.01) over different seasons.~~ During spring,

NOCs exhibit~~ed~~ a limited dependence on oxidized organics (Figs. 3a and 3b), while during

summer, the hourly detected number of NOCs show~~ed~~ a limited dependence on ammonium

(Fig. 3d). These ~~findings~~ results can be explained by ~~were consistent with~~ the PMF results,

showing that the ammonium factor explained ~80% of the predicted NOCs during spring,

while the oxidized organics factor dominantly contributed to the predicted NOCs during

warmer seasons (Fig. S8). A detailed discussion of this issue is provided in the SI.

3.~~3~~ 4 Influence of RH and ~~particle acidity~~NOx

The ~~importance~~ influence of RH on ~~NOC~~ RPAs of NOCs and peak ratios of NOCs~~ and~~

/oxidized organics, are shown in Fig. 6. While NOCs ~~did~~ do not show a clear dependence on

RH, the ratio of NOCs to oxidized organics show~~ed~~ a clear increase ~~with~~ towards higher

RH. This finding is consistent with the observations reported by Xu et al. (2017), in which

the N/C ratio significantly increase~~sd~~ as a function of RH in the atmosphere of Beijing. In

addition, the diurnal variations of NOCs with peaks values around 20:00 ~~were~~ are also

similar to those reported by Xu et al. (2017). ~~It is~~ The peak ratios of ~~noted that the formation~~

~~of NOCs~~ /~~from~~ oxidized organics ~~was~~ are more obviously ~~not~~ enhanced when RH is higher

~~conditions were lower~~ than 40%. These findings imply that aqueous-phase processing likely

plays an important role in the formation of NOCs. Significant changes in RH, such as during

the evaporation of water droplets, have been reported to facilitate the formation of NOCs via

NH_3/NH_4^+ and SOA (Nguyen et al., 2012). In addition, an increase in RH would improve

the uptake of NH_3 and formation of NH_4^+, which also contributes to the enhancement of

416 NOCs. However, the relatively weak correlation ($R^2 = 0.27$, $p < 0.01$) between the peak

417 ratios and RH, reflect the complex influence of RH on the formation of NOCs (Xu et al.,

418 2017; Woo et al., 2013). ~~It is noted that the formation of NOCs from oxidized organics was~~

419 ~~not enhanced when RH conditions were lower than 40%.~~

420   ~~While particulate organics with a high N/C ratio were formed in the presence of~~

421 ~~ammonium salts (Lee et al., 2013), the influence of particle acidity on the formation of NOCs~~

422 ~~has not previously been thoroughly evaluated. We further analyzed the influence of particle~~

423 ~~acidity on the formation of NOCs, with particle acidity represented by the relative acidity~~

424 ~~ratio, defined as the sum of absolute average peak areas of nitrate (m/z -62) and sulfate (m/z~~

425 ~~-97) divided by those of ammonium (m/z 18) (Denkenberger et al., 2007). Fig. 7 clearly~~

426 ~~shows the dependence of NOCs on particle acidity.~~ ~~Similarly, ambient observations reported~~

427 ~~from a forest site in Japan indicate that aerosol acidity likely plays an important role in the~~

428 ~~formation of WSON via acid-catalyzed reactions in summer (Miyazaki et al., 2014).~~

429 ~~Enhanced organic aerosol yields from gas-phase carbonyls in the acidic seed aerosol have~~

430 ~~been attributed to the occurrence of acid-catalyzed reactions (Jang et al., 2002). Furthermore,~~

431 ~~acidity could also play a significant role in the gas-to-particle partitioning of aldehydes~~

432 ~~(Herrmann et al., 2015; Liggio et al., 2005; Gen et al., 2018; De Haan et al., 2018; Kroll et~~

433 ~~al., 2005), although some studies have indicated that browning of some SOA occurs~~

434 ~~independently within a pH range of 4–10 (Nguyen et al., 2012).~~ ~~Consistently higher relative~~

435 ~~acidity was observed for the internally mixed ammonium and NOCs particles, as compared~~

436 ~~to ammonium-containing particles without NOCs (Fig. S7).~~ ~~This finding was consistent with~~

22

437　~~the results discussed in section 3.1, indicating that particles containing a higher abundance~~

438　~~of ammonium may not facilitate the formation of NOCs. A previously reported modelled~~

439　~~simulation showed that after including the chemistry of SOA ageing with NH_3, an increase~~

440　~~in aerosol acidity would be expected due to the reduction in NH_4, resulting in more SOA~~

441　~~generated from acid-catalyzed reactions (Zhu et al., 2018). Consequently, the relative acidity~~

442　~~ratio was also included in the multiple linear regression model applied in the present study,~~

443　~~as previously discussed. However, the inclusion of relative acidity did not improve the~~

444　~~degree of fit between the observed and modeled RPAs of NOCs. This suggests that the~~

445　~~selection of the RPAs of ammonium or the relative acidity ratio in regression analysis~~

446　~~resulted in similar outcomes for the formation of NOCs as the present study, due to the~~

447　~~overlap between these variables. Sulfate might also play a role in the enhancement of~~

448　~~formation kinetics for NOCs ($R^2 = 0.13$, $p < 0.01$), as previously demonstrated in laboratory~~

449　~~simulations showing that sulfate can enhance the partitioning of some carbonyls (Lee et al.,~~

450　~~2013).~~

451　One may expect that NOCs were formed through the interactions between NOx and

452　oxidized organics in gas phase followed by condensation (Fry et al., 2014; Stefenelli et al.,

453　2019; Lehtipalo et al., 2018). Low correlation coefficients ($R^2 = 0.02$–0.13) between NOCs

454　and NOx likely indicates limited contribution of this pathways to the observed NOCs. We

455　have also included an analysis on the relationship between peak ratios of NOCs/oxidized

456　organics and NOx. Peak area ratios of NOCs/oxidized organics generally increases with

457　increasing level of NOx (Fig. 6), but still with relatively weak correlation ($R^2 = 0.18$, $p <$

458 0.01). An inclusion of both NOx and RH in the above linear regression model (NOCs versus

459 the oxidized organics and ammonium) does not improve the prediction of NOCs ($R^2 = 0.71$,

460 $p < 0.01$). However, it is also noted that many factors (e.g., different removal processes and

461 lifetimes of particles vs. gasses, primary vs. secondary species, etc.) could contribute to a

462 lack of strong correlation even if NOx did contribute to NOC formation.

463

464 **3.4 5 Atmospheric implications and limitation**

465 In this study we showed that in an urban megacity area, secondary NOCs were

466 significantly contributed by the heterogeneous ageing of oxidized organics photochemical

467 products with NH_3/NH_4^+, providing valuable insight into SOA aging mechanisms. In

468 particular, the effects of NH_3/NH_4^+ on SOA or BrC formation remain relatively poorly

469 understood. In the PRD region, it has been shown that oxygenated organic aerosols (OOA)

470 account for more than 40% the total organic mass (He et al., 2011), with high concentrations

471 of available gaseous carbonyls (Li et al., 2014). Therefore, it is expected that over half of all

472 water soluble NOCs in this region , might link to secondary processing (Yu et al., 2017).

473 Furthermore, secondary sources have been found to contribute significantly to NOCs related

474 BrC in Nanjing, China (Chen et al., 2018). The results presented herein also suggest that the

475 production of NOCs might be effectively estimated by their correlation with secondary

476 oxidized organics and ammonium. The effectiveness of correlation- based estimations needs

477 to be examined in other regions before being generally applied in other environments.

478 However, this approach may provide valuable insights in investigations into NOCs using

24

479 atmospheric observations. In contrast, it has previously been reported that a positive

480 correlation exists between WSON and ammonium (Li et al., 2012), indicating similar

481 anthropogenic sources. This divergence could be mainly attributed to varying contributions

482 of primary sources and secondary processes to the observed NOCs. Possible future

483 reductions in anthropogenic emissions of ammonia may reduce particle NOCs.

484 Understanding the complex interplay between inorganic and organic nitrogen is an important

485 part of assessing the global nitrogen cycling.

486 Moise et al. (2015) proposed that with high concentrations of reduced nitrogen

487 compounds, high photochemical activity and frequent changes in humidity, BrC formed via

488 NH_3/NH_4^+ and SOA may become a dominant contributor to aerosol absorption, specifically

489 in agricultural and forested areas. However, this study suggests that even in typical urban

490 areas, BrC formation via NH_3/NH_4^+ and SOA should not be consideredneglected. In

491 particular, SOA was found to account for 44 – 71% of the organic mass in megacities across

492 China (Huang et al., 2014), with NH_3 concentrations in urban areas comparable with those

493 from agricultural sites and 2- or 3-fold those of forested areas in China (Pan et al., 2018).

494 Additionally, the acidic nature of particles in these regions would be also favorable for the

495 formation of NOCs (Guo et al., 2017; Jia et al., 2018).

496 Considering the formation of NOCs from the uptake of NH_3 onto SOA particles, Zhu

497 et al. (2018) suggested that this mechanism could have a significant impact on the

498 atmospheric concentrations of NH_3/NH_4^+ and NO_3^-. However, the uptake of carbonyl onto

499 the ammonium-containing particles was not considered. As discussed above, 33% of the

modelled NOCs on average could be explained by the ammonium factor, with this effect

501 most pronounced during spring (Fig. 5 and Fig. S9). Such chemistry may also result in an

502 increase in aerosol acidity due to the reduction in NH_4^+, resulting in the formation of more

503 SOA from acid-catalyzed reactions of gas phase carbonyls (Jang et al., 2002). Given that

504 RH and particle acidity play an important role in the aqueous formation of SOA and uptake

505 of NH_3, such models should be developed to include these factors, in order to improve our

506 understanding of the impact of the discussed chemical mechanisms in atmospheric chemistry

507 and the global nitrogen cycle.

508

5 Conclusions

510   This study investigated the processes contributing to the seasonal formation of NOCs,

511 involving ammonium and oxidized organics in urban Guangzhou, using single particle mass

512 spectrometry. This is the first study to provide direct field observation results to confirm that

513 the variation in of NOCs correlated well and are strongly enhanced internal mixing with

514 secondary oxidized organics. These findings highlight the possible formation pathway of

515 NOCs through ageing of secondary oxidized organics by NH_3/NH_4^+ in ambient urban

516 environments. A clear pattern of seasonal variation in NOCs was observed, with higher

517 relative contributions in summer and autumn as compared to spring and winter. This

518 seasonal variation was well predicted by multiple linear regression model analysis, using the

519 relative abundance of oxidized organics and ammonium as model inputs. More than 50% of

520 NOCs could be explained by the interaction between oxidized organics and ammonium. The

521 production of NOCs through such processes were facilitated by increased humidity and NOx

522 ~~and higher particle acidity~~. These results extend our understanding of the mixing state and

523 atmospheric processing of particulate NOCs, as well as having important implications for

524 the accuracy of models predicting the formation, fate and impacts of NOCs in the atmosphere.

525

Author contribution

527 GHZ and XHB designed the research (with input from WS, LL, ZYW, DHC, MJT, XMW

528 and GYS), analyzed the data, and wrote the manuscript. XFL, YZF and QHL conducted air

529 sampling work and laboratory experiments under the guidance of GHZ, XHB and XMW.

530 All authors contributed to the refinement of the submitted manuscript.

531

References

538

539   Aiona, P. K., Lee, H. J., Leslie, R., Lin, P., Laskin, A., Laskin, J., and Nizkorodov, S. A.:

540   Photochemistry of Products of the Aqueous Reaction of Methylglyoxal with Ammonium

541   Sulfate, Acs Earth Space Chem., 1, 522-532, doi:10.1021/acsearthspacechem.7b00075, 2017.

542   Altieri, K. E., Turpin, B. J., and Seitzinger, S. P.: Composition of Dissolved Organic

543   Nitrogen in Continental Precipitation Investigated by Ultra-High Resolution FT-ICR Mass

544   Spectrometry, Environ. Sci. Technol., 43, 6950-6955, doi:10.1021/es9007849, 2009.

545   Andreae, M. O., and Gelencser, A.: Black carbon or brown carbon? The nature of light-

546   absorbing carbonaceous aerosols, Atmos. Chem. Phys., 6, 3131-3148, 2006.

547   Bones, D. L., Henricksen, D. K., Mang, S. A., Gonsior, M., Bateman, A. P., Nguyen, T.

548   B., Cooper, W. J., and Nizkorodov, S. A.: Appearance of strong absorbers and fluorophores in

549   limonene-O-3 secondary organic aerosol due to NH4+-mediated chemical aging over long time

550   scales, J. Geophys. Res.-Atmos., 115, D05203, doi:10.1029/2009jd012864, 2010.

551   Cape, J. N., Cornell, S. E., Jickells, T. D., and Nemitz, E.: Organic nitrogen in the

552   atmosphere — Where does it come from? A review of sources and methods, Atmos. Res., 102,

553   30-48, doi:10.1016/j.atmosres.2011.07.009, 2011.

554   Chen, Y., Ge, X., Chen, H., Xie, X., Chen, Y., Wang, J., Ye, Z., Bao, M., Zhang, Y., and

555   Chen, M.: Seasonal light absorption properties of water-soluble brown carbon in atmospheric

556   fine particles in Nanjing, China, Atmos. Environ., doi:10.1016/j.atmosenv.2018.06.002, 2018.

557   Chu, B. W., Zhang, X., Liu, Y. C., He, H., Sun, Y., Jiang, J. K., Li, J. H., and Hao, J. M.:

558   Synergetic formation of secondary inorganic and organic aerosol: effect of SO2 and NH3 on

559   particle formation and growth, Atmos. Chem. Phys., 16, 14219-14230, doi:10.5194/acp-16-

560   14219-2016, 2016.

561   De Gouw, J., and Jimenez, J. L.: Organic Aerosols in the Earth's Atmosphere, Environ.

562   Sci. Technol., 43, 7614-7618, doi:10.1021/Es9006004, 2009.

563   De Haan, D. O., Hawkins, L. N., Kononenko, J. A., Turley, J. J., Corrigan, A. L., Tolbert,

564   M. A., and Jimenez, J. L.: Formation of Nitrogen-Containing Oligomers by Methylglyoxal and

565 Amines in Simulated Evaporating Cloud Droplets, Environ. Sci. Technol., 45, 984-991,

566 doi:10.1021/es102933x, 2011.

567 De Haan, D. O., Hawkins, L. N., Welsh, H. G., Pednekar, R., Casar, J. R., Pennington, E.

568 A., de Loera, A., Jimenez, N. G., Symons, M. A., Zauscher, M., Pajunoja, A., Caponi, L.,

569 Cazaunau, M., Formenti, P., Gratien, A., Pangui, E., and Doussin, J.-F.: Brown Carbon

570 Production in Ammonium- or Amine-Containing Aerosol Particles by Reactive Uptake of

571 Methylglyoxal and Photolytic Cloud Cycling, Environ. Sci. Technol., 51, 7458-7466,

572 doi:10.1021/acs.est.7b00159, 2017.

573 De Haan, D. O., Jimenez, N. G., de Loera, A., Cazaunau, M., Gratien, A., Pangui, E., and

574 Doussin, J.-F.: Methylglyoxal Uptake Coefficients on Aqueous Aerosol Surfaces, J. Phys.

575 Chem. A, 122, 4854-4860, doi:10.1021/acs.jpca.8b00533, 2018.

576 Denkenberger, K. A., Moffet, R. C., Holecek, J. C., Rebotier, T. P., and Prather, K. A.:

577 Real-time, single-particle measurements of oligomers in aged ambient aerosol particles,

578 Environ. Sci. Technol., 41, 5439-5446, doi:10.1021/es070329l, 2007.

579 Desyaterik, Y., Sun, Y., Shen, X., Lee, T., Wang, X., Wang, T., and Collett, J. L., Jr.:

580 Speciation of "brown" carbon in cloud water impacted by agricultural biomass burning in

581 eastern China, J. Geophys. Res.-Atmos., 118, 7389-7399, doi:10.1002/jgrd.50561, 2013.

582 El-Sayed, M. M. H., Wang, Y. Q., and Hennigan, C. J.: Direct atmospheric evidence for

583 the irreversible formation of aqueous secondary organic aerosol, Geophys. Res. Lett., 42, 5577-

584 5586, doi:10.1002/2015gl064556, 2015.

585 Feng, Y., Ramanathan, V., and Kotamarthi, V. R.: Brown carbon: a significant

586 atmospheric absorber of solar radiation?, Atmos. Chem. Phys., 13, 8607-8621,

587 doi:10.5194/acp-13-8607-2013, 2013.

588 Fry, J. L., Draper, D. C., Barsanti, K. C., Smith, J. N., Ortega, J., Winkle, P. M., Lawler,

589 M. J., Brown, S. S., Edwards, P. M., Cohen, R. C., and Lee, L.: Secondary Organic Aerosol

590 Formation and Organic Nitrate Yield from NO3 Oxidation of Biogenic Hydrocarbons, Environ.

591 Sci. Technol., 48, 11944-11953, doi:10.1021/es502204x, 2014.

592   Galloway, M. M., Chhabra, P. S., Chan, A. W. H., Surratt, J. D., Flagan, R. C., Seinfeld,
593   J. H., and Keutsch, F. N.: Glyoxal uptake on ammonium sulphate seed aerosol: reaction
594   products and reversibility of uptake under dark and irradiated conditions, Atmos. Chem. Phys.,
595   9, 3331-3345, doi:10.5194/acp-9-3331-2009, 2009.

596   Gen, M., Huang, D. D., and Chan, C. K.: Reactive Uptake of Glyoxal by Ammonium-
597   Containing Salt Particles as a Function of Relative Humidity, Environ. Sci. Technol., 52, 6903-
598   6911, doi:10.1021/acs.est.8b00606, 2018.

599   Guo, H., Xu, L., Bougiatioti, A., Cerully, K. M., Capps, S. L., Hite, J. R., Carlton, A. G.,
600   Lee, S. H., Bergin, M. H., Ng, N. L., Nenes, A., and Weber, R. J.: Fine-particle water and pH
601   in the southeastern United States, Atmos. Chem. Phys., 15, 5211-5228, doi:10.5194/acp-15-
602   5211-2015, 2015.

603   Guo, H., Weber, R. J., and Nenes, A.: High levels of ammonia do not raise fine particle
604   pH sufficiently to yield nitrogen oxide-dominated sulfate production, Sci. Rep., 7, 12109,
605   doi:10.1038/s41598-017-11704-0, 2017.

606   Hawkins, L. N., Lemire, A. N., Galloway, M. M., Corrigan, A. L., Turley, J. J., Espelien,
607   B. M., and De Haan, D. O.: Maillard Chemistry in Clouds and Aqueous Aerosol As a Source
608   of Atmospheric Humic-Like Substances, Environ. Sci. Technol., 50, 7443-7452,
609   doi:10.1021/acs.est.6b00909, 2016.

610   He, L. Y., Huang, X. F., Xue, L., Hu, M., Lin, Y., Zheng, J., Zhang, R. Y., and Zhang, Y.
611   H.: Submicron aerosol analysis and organic source apportionment in an urban atmosphere in
612   Pearl River Delta of China using high-resolution aerosol mass spectrometry, J. Geophys. Res.-
613   Atmos., 116, 1-15, doi:10.1029/2010jd014566, 2011.

614   Healy, R. M., Sciare, J., Poulain, L., Crippa, M., Wiedensohler, A., Prevot, A. S. H.,
615   Baltensperger, U., Sarda-Esteve, R., McGuire, M. L., Jeong, C. H., McGillicuddy, E., O'Connor,
616   I. P., Sodeau, J. R., Evans, G. J., and Wenger, J. C.: Quantitative determination of carbonaceous
617   particle mixing state in Paris using single-particle mass spectrometer and aerosol mass
618   spectrometer measurements, Atmos. Chem. Phys., 13, 9479-9496, doi:10.5194/acp-13-9479-
619   2013, 2013.

620   Hennigan, C. J., Izumi, J., Sullivan, A. P., Weber, R. J., and Nenes, A.: A critical
621   evaluation of proxy methods used to estimate the acidity of atmospheric particles, Atmos. Chem.
622   Phys., 15, 2775-2790, doi:10.5194/acp-15-2775-2015, 2015.

623   Herrmann, H., Schaefer, T., Tilgner, A., Styler, S. A., Weller, C., Teich, M., and Otto, T.:
624   Tropospheric Aqueous-Phase Chemistry: Kinetics, Mechanisms, and Its Coupling to a
625   Changing Gas Phase, Chem. Rev., 115, 4259-4334, doi:10.1021/cr500447k, 2015.

626   Ho, K. F., Ho, S. S. H., Lee, S. C., Kawamura, K., Zou, S. C., Cao, J. J., and Xu, H. M.:
627   Summer and winter variations of dicarboxylic acids, fatty acids and benzoic acid in PM2.5 in
628   Pearl Delta River Region, China, Atmos. Chem. Phys., 11, 2197-2208, doi:10.5194/acp-11-
629   2197-2011, 2011.

630   Ho, K. F., Ho, S. S. H., Huang, R. J., Liu, S. X., Cao, J. J., Zhang, T., Chuang, H. C., Chan,
631   C. S., Hu, D., and Tian, L. W.: Characteristics of water-soluble organic nitrogen in fine
632   particulate matter in the continental area of China, Atmos. Environ., 106, 252-261,
633   doi:10.1016/j.atmosenv.2015.02.010, 2015.

634   Hu, M., Wu, Z., Slanina, J., Lin, P., Liu, S., and Zeng, L.: Acidic gases, ammonia and
635   water-soluble ions in PM2.5 at a coastal site in the Pearl River Delta, China, Atmos. Environ.,
636   42, 6310-6320, 2008.

637   Huang, M., Xu, J., Cai, S., Liu, X., Zhao, W., Hu, C., Gu, X., Fang, L., and Zhang, W.:
638   Characterization of brown carbon constituents of benzene secondary organic aerosol aged with
639   ammonia, J. Atmos. Chem., 75, 205-218, doi:10.1007/s10874-017-9372-x, 2017.

640   Huang, R. J., Zhang, Y., Bozzetti, C., Ho, K. F., Cao, J. J., Han, Y., Daellenbach, K. R.,
641   Slowik, J. G., Platt, S. M., Canonaco, F., Zotter, P., Wolf, R., Pieber, S. M., Bruns, E. A., Crippa,
642   M., Ciarelli, G., Piazzalunga, A., Schwikowski, M., Abbaszade, G., Schnelle-Kreis, J.,
643   Zimmermann, R., An, Z., Szidat, S., Baltensperger, U., El Haddad, I., and Prevot, A. S.: High
644   secondary aerosol contribution to particulate pollution during haze events in China, Nature, 514,
645   218-222, doi:10.1038/nature13774, 2014.

646   Jeong, C. H., McGuire, M. L., Godri, K. J., Slowik, J. G., Rehbein, P. J. G., and Evans, G.

647   J.: Quantification of aerosol chemical composition using continuous single particle

648   measurements, Atmos. Chem. Phys., 11, 7027-7044, doi:10.5194/acp-11-7027-2011, 2011.

649   Jia, S. G., Sarkar, S., Zhang, Q., Wang, X. M., Wu, L. L., Chen, W. H., Huang, M. J.,

650   Zhou, S. Z., Zhang, J. P., Yuan, L., and Yang, L. M.: Characterization of diurnal variations of

651   PM2.5 acidity using an open thermodynamic system: A case study of Guangzhou, China,

652   Chemosphere, 202, 677-685, doi:10.1016/j.chemosphere.2018.03.127, 2018.

653   Kampf, C. J., Filippi, A., Zuth, C., Hoffmann, T., and Opatz, T.: Secondary brown carbon

654   formation via the dicarbonyl imine pathway: nitrogen heterocycle formation and synergistic

655   effects, Phys. Chem. Chem. Phys., 18, 18353-18364, doi:10.1039/c6cp03029g, 2016.

656   Kanakidou, M., Seinfeld, J. H., Pandis, S. N., Barnes, I., Dentener, F. J., Facchini, M. C.,

657   Van Dingenen, R., Ervens, B., Nenes, A., Nielsen, C. J., Swietlicki, E., Putaud, J. P., Balkanski,

658   Y., Fuzzi, S., Horth, J., Moortgat, G. K., Winterhalter, R., Myhre, C. E. L., Tsigaridis, K.,

659   Vignati, E., Stephanou, E. G., and Wilson, J.: Organic aerosol and global climate modelling: a

660   review, Atmos. Chem. Phys., 5, 1053-1123, 2005.

661   Kroll, J. H., Ng, N. L., Murphy, S. M., Varutbangkul, V., Flagan, R. C., and Seinfeld, J.

662   H.: Chamber studies of secondary organic aerosol growth by reactive uptake of simple carbonyl

663   compounds, J. Geophys. Res.-Atmos., 110, doi:10.1029/2005JD006004, 2005.

664   Laskin, A., Smith, J. S., and Laskin, J.: Molecular Characterization of Nitrogen-

665   Containing Organic Compounds in Biomass Burning Aerosols Using High-Resolution Mass

666   Spectrometry, Environ. Sci. Technol., 43, 3764-3771, doi:10.1021/es803456n, 2009.

667   Laskin, A., Laskin, J., and Nizkorodov, S. A.: Chemistry of Atmospheric Brown Carbon,

668   Chem. Rev., 115, 4335-4382, doi:10.1021/cr5006167, 2015.

669   Lee, A. K. Y., Zhao, R., Li, R., Liggio, J., Li, S. M., and Abbatt, J. P. D.: Formation of

670   Light Absorbing Organo-Nitrogen Species from Evaporation of Droplets Containing Glyoxal

671   and Ammonium Sulfate, Environ. Sci. Technol., 47, 12819-12826, doi:10.1021/es402687w,

672   2013.

673   Lee, S. H., Murphy, D. M., Thomson, D. S., and Middlebrook, A. M.: Nitrate and oxidized

674   organic ions in single particle mass spectra during the 1999 Atlanta Supersite Project, J.

675   Geophys. Res., 108, 8417, doi:10.1029/2001jd001455, 2003.

676   Lehtipalo, K., Yan, C., Dada, L., Bianchi, F., Xiao, M., Wagner, R., Stolzenburg, D.,

677   Ahonen, L. R., Amorim, A., Baccarini, A., Bauer, P. S., Baumgartner, B., Bergen, A.,

678   Bernhammer, A.-K., Breitenlechner, M., Brilke, S., Buchholz, A., Mazon, S. B., Chen, D., Chen,

679   X., Dias, A., Dommen, J., Draper, D. C., Duplissy, J., Ehn, M., Finkenzeller, H., Fischer, L.,

680   Frege, C., Fuchs, C., Garmash, O., Gordon, H., Hakala, J., He, X., Heikkinen, L., Heinritzi, M.,

681   Helm, J. C., Hofbauer, V., Hoyle, C. R., Jokinen, T., Kangasluoma, J., Kerminen, V.-M., Kim,

682   C., Kirkby, J., Kontkanen, J., Kürten, A., Lawler, M. J., Mai, H., Mathot, S., Mauldin, R. L.,

683   Molteni, U., Nichman, L., Nie, W., Nieminen, T., Ojdanic, A., Onnela, A., Passananti, M.,

684   Petäjä, T., Piel, F., Pospisilova, V., Quéléver, L. L. J., Rissanen, M. P., Rose, C., Sarnela, N.,

685   Schallhart, S., Schuchmann, S., Sengupta, K., Simon, M., Sipilä, M., Tauber, C., Tomé, A.,

686   Tröstl, J., Väisänen, O., Vogel, A. L., Volkamer, R., Wagner, A. C., Wang, M., Weitz, L.,

687   Wimmer, D., Ye, P., Ylisirniö, A., Zha, Q., Carslaw, K. S., Curtius, J., Donahue, N. M., Flagan,

688   R. C., Hansel, A., Riipinen, I., Virtanen, A., Winkler, P. M., Baltensperger, U., Kulmala, M.,

689   and Worsnop, D. R.: Multicomponent new particle formation from sulfuric acid, ammonia, and

690   biogenic vapors, Sci. Adv., 4, eaau5363, doi:10.1126/sciadv.aau5363, 2018.

691   Li, J., Fang, Y. T., Yoh, M., Wang, X. M., Wu, Z. Y., Kuang, Y. W., and Wen, D. Z.:

692   Organic nitrogen deposition in precipitation in metropolitan Guangzhou city of southern China,

693   Atmos. Res., 113, 57-67, doi:10.1016/j.atmosres.2012.04.019, 2012.

694   Li, L., Huang, Z. X., Dong, J. G., Li, M., Gao, W., Nian, H. Q., Fu, Z., Zhang, G. H., Bi,

695   X. H., Cheng, P., and Zhou, Z.: Real time bipolar time-of-flight mass spectrometer for analyzing

696   single aerosol particles, Intl. J. Mass. Spectrom., 303, 118-124, doi:10.1016/j.ijms.2011.01.017,

697   2011.

698   Li, X., Rohrer, F., Brauers, T., Hofzumahaus, A., Lu, K., Shao, M., Zhang, Y. H., and

699   Wahner, A.: Modeling of HCHO and CHOCHO at a semi-rural site in southern China during

700   the PRIDE-PRD2006 campaign, Atmos. Chem. Phys., 14, 12291-12305, doi:10.5194/acp-14-
701   12291-2014, 2014.

702   Li, Z. J., Nizkorodov, S. A., Chen, H., Lu, X. H., Yang, X., and Chen, J. M.: Nitrogen-
703   containing secondary organic aerosol formation by acrolein reaction with ammonia/ammonium,
704   Atmos. Chem. Phys., 19, 1343-1356, doi:10.5194/acp-19-1343-2019, 2019.

705   Liggio, J., Li, S. M., and Mclaren, R.: Reactive uptake of glyoxal by particulate matter, J.
706   Geophys. Res.-Atmos., 110, doi:10.1029/2004jd005113, 2005.

707   Lin, P., Aiona, P. K., Li, Y., Shiraiwa, M., Laskin, J., Nizkorodov, S. A., and Laskin, A.:
708   Molecular Characterization of Brown Carbon in Biomass Burning Aerosol Particles, Environ.
709   Sci. Technol., 50, 11815-11824, doi:10.1021/acs.est.6603024, 2016.

710   Liu, Y., Liggio, J., Staebler, R., and Li, S. M.: Reactive uptake of ammonia to secondary
711   organic aerosols: kinetics of organonitrogen formation, Atmos. Chem. Phys., 15, 13569-13584,
712   doi:10.5194/acp-15-13569-2015, 2015.

713   Mace, K. A., Kubilay, N., and Duce, R. A.: Organic nitrogen in rain and aerosol in the
714   eastern Mediterranean atmosphere: An association with atmospheric dust, J. Geophys. Res.-
715   Atmos., 108, doi:10.1029/2002jd002997, 2003.

716   Mang, S. A., Henricksen, D. K., Bateman, A. P., Andersen, M. P. S., Blake, D. R., and
717   Nizkorodov, S. A.: Contribution of Carbonyl Photochemistry to Aging of Atmospheric
718   Secondary Organic Aerosol, J. Phys. Chem. A, 112, 8337-8344, doi:10.1021/jp804376c, 2008.

719   Miyazaki, Y., Fu, P. Q., Ono, K., Tachibana, E., and Kawamura, K.: Seasonal cycles of
720   water-soluble organic nitrogen aerosols in a deciduous broadleaf forest in northern Japan, J.
721   Geophys. Res.-Atmos., 119, 1440-1454, doi:10.1002/2013JD020713, 2014.

722   Mohr, C., Lopez-Hilfiker, F. D., Zotter, P., Prévôt, A. S. H., Xu, L., Ng, N. L., Herndon,
723   S. C., Williams, L. R., Franklin, J. P., Zahniser, M. S., Worsnop, D. R., Knighton, W. B., Aiken,
724   A. C., Gorkowski, K. J., Dubey, M. K., Allan, J. D., and Thornton, J. A.: Contribution of
725   Nitrated Phenols to Wood Burning Brown Carbon Light Absorption in Detling, United
726   Kingdom during Winter Time, Environ. Sci. Technol., 47, 6316-6324, doi:10.1021/es400683v,
727   2013.

728   Moise, T., Flores, J. M., and Rudich, Y.: Optical Properties of Secondary Organic Aerosols
729   and Their Changes by Chemical Processes, Chem. Rev., 115, 4400-4439,
730   doi:10.1021/cr5005259, 2015.

731   Murphy, J. G., Gregoire, P. K., Tevlin, A. G., Wentworth, G. R., Ellis, R. A., Markovic,
732   M. Z., and VandenBoer, T. C.: Observational constraints on particle acidity using
733   measurements and modelling of particles and gases, Faraday Discuss., 200, 379-395,
734   doi:10.1039/c7fd00086c, 2017.

735   Neff, J. C., Holland, E. A., Dentener, F. J., McDowell, W. H., and Russell, K. M.: The
736   origin, composition and rates of organic nitrogen deposition: A missing piece of the nitrogen
737   cycle?, Biogeochemistry, 57, 99-136, 2002.

738   Nguyen, T. B., Lee, P. B., Updyke, K. M., Bones, D. L., Laskin, J., Laskin, A., and
739   Nizkorodov, S. A.: Formation of nitrogen- and sulfur-containing light-absorbing compounds
740   accelerated by evaporation of water from secondary organic aerosols, J. Geophys. Res.-Atmos.,
741   117, D01207, doi:10.1029/2011jd016944, 2012.

742   Norris, G., Vedantham, R., Wade, K., Zahn, P., Brown, S., Paatero, P., Eberly, S., and
743   Foley, C. (2009), Guidance document for PMF applications with the Multilinear Engine, edited,
744   Prepared for the U.S. Environmental Protection Agency, Research Triangle Park, NC.

745   Noziere, B., Dziedzic, P., and Cordova, A.: Products and Kinetics of the Liquid-Phase
746   Reaction of Glyoxal Catalyzed by Ammonium Ions (NH4+), J. Phys. Chem. A, 113, 231-237,
747   doi:10.1021/jp8078293, 2009.

748   Noziere, B., Kaberer, M., Claeys, M., Allan, J., D'Anna, B., Decesari, S., Finessi, E.,
749   Glasius, M., Grgic, I., Hamilton, J. F., Hoffmann, T., Iinuma, Y., Jaoui, M., Kahno, A., Kampf,
750   C. J., Kourtchev, I., Maenhaut, W., Marsden, N., Saarikoski, S., Schnelle-Kreis, J., Surratt, J.
751   D., Szidat, S., Szmigielski, R., and Wisthaler, A.: The Molecular Identification of Organic
752   Compounds in the Atmosphere: State of the Art and Challenges, Chem. Rev., 115, 3919-3983,
753   doi:10.1021/cr5003485, 2015.

754   Pagels, J., Dutcher, D. D., Stolzenburg, M. R., McMurry, P. H., Galli, M. E., and Gross,
755   D. S.: Fine-particle emissions from solid biofuel combustion studied with single-particle mass

756 spectrometry: Identification of markers for organics, soot, and ash components, J. Geophys.

757 Res.-Atmos., 118, 859-870, doi:10.1029/2012jd018389, 2013.

758 Pan, Y. P., Tian, S. L., Zhao, Y. H., Zhang, L., Zhu, X. Y., Gao, J., Huang, W., Zhou, Y.

759 B., Song, Y., Zhang, Q., and Wang, Y. S.: Identifying Ammonia Hotspots in China Using a

760 National Observation Network, Environ. Sci. Technol., 52, 3926-3934,

761 doi:10.1021/acs.est.7b05235, 2018.

762 Paulot, F., Wunch, D., Crounse, J. D., Toon, G. C., Millet, D. B., DeCarlo, P. F.,

763 Vigouroux, C., Deutscher, N. M., González Abad, G., Notholt, J., Warneke, T., Hannigan, J.

764 W., Warneke, C., de Gouw, J. A., Dunlea, E. J., De Mazière, M., Griffith, D. W. T., Bernath,

765 P., Jimenez, J. L., and Wennberg, P. O.: Importance of secondary sources in the atmospheric

766 budgets of formic and acetic acids, Atmos. Chem. Phys., 11, 1989-2013, doi:10.5194/acp-11-

767 1989-2011, 2011.

768 Qin, X. Y., Bhave, P. V., and Prather, K. A.: Comparison of two methods for obtaining

769 quantitative mass concentrations from aerosol time-of-flight mass spectrometry measurements,

770 Anal. Chem., 78, 6169-6178, doi:10.1021/ac060395q, 2006.

771 Rastogi, N., Zhang, X., Edgerton, E. S., Ingall, E., and Weber, R. J.: Filterable water-

772 soluble organic nitrogen in fine particles over the southeastern USA during summer, Atmos.

773 Environ., 45, 6040-6047, doi:10.1016/j.atmosenv.2011.07.045, 2011.

774 Sareen, N., Schwier, A. N., Shapiro, E. L., Mitroo, D., and McNeill, V. F.: Secondary

775 organic material formed by methylglyoxal in aqueous aerosol mimics, Atmos. Chem. Phys., 10,

776 997-1016, doi:10.5194/acp-10-997-2010, 2010.

777 Shapiro, E. L., Szprengiel, J., Sareen, N., Jen, C. N., Giordano, M. R., and McNeill, V. F.:

778 Light-absorbing secondary organic material formed by glyoxal in aqueous aerosol mimics,

779 Atmos. Chem. Phys., 9, 2289-2300, 2009.

780 Shi, J., Gao, H., Qi, J., Zhang, J., and Yao, X.: Sources, compositions, and distributions of

781 water-soluble organic nitrogen in aerosols over the China Sea, J. Geophys. Res.-Atmos., 115,

782 doi:10.1029/2009jd013238, 2010.

783   Shrivastava, M., Cappa, C. D., Fan, J. W., Goldstein, A. H., Guenther, A. B., Jimenez, J.

784   L., Kuang, C., Laskin, A., Martin, S. T., Ng, N. L., Petaja, T., Pierce, J. R., Rasch, P. J., Roldin,

785   P., Seinfeld, J. H., Shilling, J., Smith, J. N., Thornton, J. A., Volkamer, R., Wang, J., Worsnop,

786   D. R., Zaveri, R. A., Zelenyuk, A., and Zhang, Q.: Recent advances in understanding secondary

787   organic aerosol: Implications for global climate forcing, Rev. Geophys., 55, 509-559,

788   doi:10.1002/2016RG000540, 2017.

789   Silva, P. J., and Prather, K. A.: Interpretation of mass spectra from organic compounds in

790   aerosol time-of-flight mass spectrometry, Anal. Chem., 72, 3553-3562, 2000.

791   Stefenelli, G., Pospisilova, V., Lopez-Hilfiker, F. D., Daellenbach, K. R., Hüglin, C., Tong,

792   Y., Baltensperger, U., Prevot, A. S. H., and Slowik, J. G.: Organic aerosol source apportionment

793   in Zurich using extractive electrospray ionization time-of-flight mass spectrometry (EESI-TOF):

794   Part I, biogenic influences and day/night chemistry in summer, Atmos. Chem. Phys. Discuss.,

795   2019, 1-36, doi:10.5194/acp-2019-361, 2019.

796   Sullivan, R. C., and Prather, K. A.: Investigations of the diurnal cycle and mixing state of

797   oxalic acid in individual particles in Asian aerosol outflow, Environ. Sci. Technol., 41, 8062-

798   8069, 2007.

799   Sun, J. Z., Zhi, G. R., Hitzenberger, R., Chen, Y. J., Tian, C. G., Zhang, Y. Y., Feng, Y.

800   L., Cheng, M. M., Zhang, Y. Z., Cai, J., Chen, F., Qiu, Y., Jiang, Z., Li, J., Zhang, G., and Mo,

801   Y.: Emission factors and light absorption properties of brown carbon from household coal

802   combustion in China, Atmos. Chem. Phys., 17, 4769-4780, doi:10.5194/acp-17-4769-2017,

803   2017.

804   Sun, Y. L., Zhang, Q., Schwab, J. J., Demerjian, K. L., Chen, W. N., Bae, M. S., Hung, H.

805   M., Hogrefe, O., Frank, B., Rattigan, O. V., and Lin, Y. C.: Characterization of the sources and

806   processes of organic and inorganic aerosols in New York city with a high-resolution time-of-

807   flight aerosol mass apectrometer, Atmos. Chem. Phys., 11, 1581-1602, doi:10.5194/acp-11-

808   1581-2011, 2011.

809   Updyke, K. M., Nguyen, T. B., and Nizkorodov, S. A.: Formation of brown carbon via

810   reactions of ammonia with secondary organic aerosols from biogenic and anthropogenic

811   precursors, Atmos. Environ., 63, 22-31, doi:10.1016/j.atmosenv.2012.09.012, 2012.

812   Wang, X. F., Gao, S., Yang, X., Chen, H., Chen, J. M., Zhuang, G. S., Surratt, J. D., Chan,

813   M. N., and Seinfeld, J. H.: Evidence for High Molecular Weight Nitrogen-Containing Organic

814   Salts in Urban Aerosols, Environ. Sci. Technol., 44, 4441-4446, 2010.

815   Wang, X. F., Wang, H. L., Jing, H., Wang, W. N., Cui, W. D., Williams, B. J., and Biswas,

816   P.: Formation of Nitrogen-Containing Organic Aerosol during Combustion of High-Sulfur-

817   Content Coal, Energ. Fuel., 31, 14161-14168, doi:10.1021/acs.energyfuels.7b02273, 2017.

818   Woo, J. L., Kim, D. D., Schwier, A. N., Li, R. Z., and McNeill, V. F.: Aqueous aerosol

819   SOA formation: impact on aerosol physical properties, Faraday Discuss., 165, 357-367,

820   doi:10.1039/c3fd00032j, 2013.

821   Xu, W. Q., Sun, Y. L., Wang, Q. Q., Du, W., Zhao, J., Ge, X. L., Han, T. T., Zhang, Y. J.,

822   Zhou, W., Li, J., Fu, P. Q., Wang, Z. F., and Worsnop, D. R.: Seasonal Characterization of

823   Organic Nitrogen in Atmospheric Aerosols Using High Resolution Aerosol Mass Spectrometry

824   in   Beijing,   China,   Acs   Earth   Space   Chem.,   1,   673-682,

825   doi:10.1021/acsearthspacechem.7b00106, 2017.

826   Yan, J., Wang, X., Gong, P., Wang, C., and Cong, Z.: Review of brown carbon aerosols:

827   Recent   progress   and   perspectives,   Sci.   Total.   Environ.,   634,   1475-1485,

828   doi:10.1016/j.scitotenv.2018.04.083, 2018.

829   Yu, X., Yu, Q. Q., Zhu, M., Tang, M. J., Li, S., Yang, W. Q., Zhang, Y. L., Deng, W., Li,

830   G. H., Yu, Y. G., Huang, Z. H., Song, W., Ding, X., Hu, Q. H., Li, J., Bi, X. H., and Wang, X.

831   M.: Water Soluble Organic Nitrogen (WSON) in Ambient Fine Particles Over a Megacity in

832   South China: Spatiotemporal Variations and Source Apportionment, J. Geophys. Res.-Atmos.,

833   122, 13045-13060, doi:10.1002/2017JD027327, 2017.

834   Yuan, B., Liggio, J., Wentzell, J., Li, S. M., Stark, H., Roberts, J. M., Gilman, J., Lerner,

835   B., Warneke, C., Li, R., Leithead, A., Osthoff, H. D., Wild, R., Brown, S. S., and de Gouw, J.

836   A.: Secondary formation of nitrated phenols: insights from observations during the Uintah

837 BasinWinter Ozone Study (UBWOS) 2014, Atmos. Chem. Phys., 16, 2139-2153,
838 doi:10.5194/acp-16-2139-2016, 2016.

839 Yuan, Q., Lai, S., Song, J., Ding, X., Zheng, L., Wang, X., Zhao, Y., Zheng, J., Yue, D.,
840 Zhong, L., Niu, X., and Zhang, Y.: Seasonal cycles of secondary organic aerosol tracers in rural
841 Guangzhou, Southern China: The importance of atmospheric oxidants, Environ. Pollut., 240,
842 884-893, doi:10.1016/j.envpol.2018.05.009, 2018.

843 Zauscher, M. D., Wang, Y., Moore, M. J. K., Gaston, C. J., and Prather, K. A.: Air Quality
844 Impact and Physicochemical Aging of Biomass Burning Aerosols during the 2007 San Diego
845 Wildfires, Environ. Sci. Technol., 47, 7633-7643, doi:10.1021/es4004137, 2013.

846 Zawadowicz, M. A., Froyd, K. D., Murphy, D. M., and Cziczo, D. J.: Improved
847 identification of primary biological aerosol particles using single-particle mass spectrometry,
848 Atmos. Chem. Phys., 17, 7193-7212, doi:10.5194/acp-17-7193-2017, 2017.

849 Zhang, G., Lin, Q., Peng, L., Yang, Y., Jiang, F., Liu, F., Song, W., Chen, D., Cai, Z., Bi,
850 X., Miller, M., Tang, M., Huang, W., Wang, X., Peng, P., and Sheng, G.: Oxalate Formation
851 Enhanced by Fe-Containing Particles and Environmental Implications, Environ. Sci. Technol.,
852 53, 1269-1277, doi:10.1021/acs.est.8b05280, 2019.

853 Zhang, G. H., Bi, X. H., He, J. J., Chen, D. H., Chan, L. Y., Xie, G. W., Wang, X. M.,
854 Sheng, G. Y., Fu, J. M., and Zhou, Z.: Variation of secondary coatings associated with
855 elemental carbon by single particle analysis, Atmos. Environ., 92, 162-170,
856 doi:10.1016/j.atmosenv.2014.04.018, 2014.

857 Zhang, G. H., Lin, Q. H., Peng, L., Yang, Y. X., Fu, Y. Z., Bi, X. H., Li, M., Chen, D. H.,
858 Chen, J. X., Cai, Z., Wang, X. M., Peng, P. A., Sheng, G. Y., and Zhou, Z.: Insight into the in-
859 cloud formation of oxalate based on in situ measurement by single particle mass spectrometry,
860 Atmos. Chem. Phys., 17, 13891-13901, doi:10.5194/acp-17-13891-2017, 2017.

861 Zhang, Q., Duan, F., He, K., Ma, Y., Li, H., Kimoto, T., and Zheng, A.: Organic nitrogen
862 in PM2.5 in Beijing, Frontiers of Environmental Science & Engineering, 9, 1004-1014,
863 doi:10.1007/s11783-015-0799-5, 2015.

864   Zhang, Y. S., Shao, M., Lin, Y., Luan, S. J., Mao, N., Chen, W. T., and Wang, M.:

865   Emission inventory of carbonaceous pollutants from biomass burning in the Pearl River Delta

866   Region, China, Atmos. Environ., 76, 189-199, doi:10.1016/j.atmosenv.2012.05.055, 2013.

867   Zhao, R., Lee, A. K. Y., and Abbatt, J. P. D.: Investigation of Aqueous-Phase

868   Photooxidation of Glyoxal and Methylglyoxal by Aerosol Chemical Ionization Mass

869   Spectrometry: Observation of Hydroxyhydroperoxide Formation, J. Phys. Chem. A, 116, 6253-

870   6263, doi:10.1021/jp211528d, 2012.

871   Zhao, R., Lee, A. K. Y., Huang, L., Li, X., Yang, F., and Abbatt, J. P. D.: Photochemical

872   processing of aqueous atmospheric brown carbon, Atmos. Chem. Phys., 15, 6087-6100,

873   doi:10.5194/acp-15-6087-2015, 2015.

874   Zheng, J. Y., Yin, S. S., Kang, D. W., Che, W. W., and Zhong, L. J.: Development and

875   uncertainty analysis of a high-resolution NH3 emissions inventory and its implications with

876   precipitation over the Pearl River Delta region, China, Atmos. Chem. Phys., 12, 7041-7058,

877   doi:10.5194/acp-12-7041-2012, 2012.

878   Zhou, S. Z., Wang, T., Wang, Z., Li, W. J., Xu, Z., Wang, X. F., Yuan, C., Poon, C. N.,

879   Louie, P. K. K., Luk, C. W. Y., and Wang, W. X.: Photochemical evolution of organic aerosols

880   observed in urban plumes from Hong Kong and the Pearl River Delta of China, Atmos. Environ.,

881   88, 219-229, doi:10.1016/j.atmosenv.2014.01.032, 2014.

882   Zhou, Y., Huang, X. H. H., Griffith, S. M., Li, M., Li, L., Zhou, Z., Wu, C., Meng, J. W.,

883   Chan, C. K., Louie, P. K. K., and Yu, J. Z.: A field measurement based scaling approach for

884   quantification of major ions, organic carbon, and elemental carbon using a single particle

885   aerosol   mass   spectrometer,   Atmos.   Environ.,   143,   300-312,

886   doi:10.1016/j.atmosenv.2016.08.054, 2016.

887   Zhu, S. P., Horne, J. R., Montoya-Aguilera, J., Hinks, M. L., Nizkorodov, S. A., and

888   Dabdub, D.: Modeling reactive ammonia uptake by secondary organic aerosol in CMAQ:

889   application to the continental US, Atmos. Chem. Phys., 18, 3641-3657, doi:10.5194/acp-18-

890   3641-2018, 2018.

891

Figure captions

892

893   Figure 1. Representative mass spectrum for NOCs-containing particles. The ion

894   peaks corresponding to NOCs and oxidized organics are highlighted with red bars.

895   Figure 2. The variation in hourly mean Nfs of the oxidized organics and

896   ammonium that internally mixed with NOCs. Box and whisker plot shows lower,

897   median and upper lines, denoting the 25th, 50th and 75th percentiles, respectively; the

898   lower and upper edges denote the 10th and 90th percentiles, respectively.

899   Figure 3. Correlation analysis of (a, c) the RPAs and (b, d) the number of

900   detected NOCs, with the oxidized organics and ammonium in different seasons.

901   Significant ($p < 0.01$) correlations were obtained for both the total observed data and

902   the seasonally separated data. RPA is defined as the fractional peak area of each m/z

903   relative to the sum of peak areas in the mass spectrum and is applied to represent the

904   relative amount of a species on a particle (Jeong et al., 2011; Healy et al., 2013).

905   Figure 4. Comparison between the measured and predicted RPAs for NOCs.

906   Figure 5. (left) PMF-resolved 3-factor source profiles (percentage of total species)

907   and (right) their diurnal variation (arbitrary unit).

908   Figure 6. The dependence of NOCs and the ratio of NOCs to the oxidized organics

909   on RH.
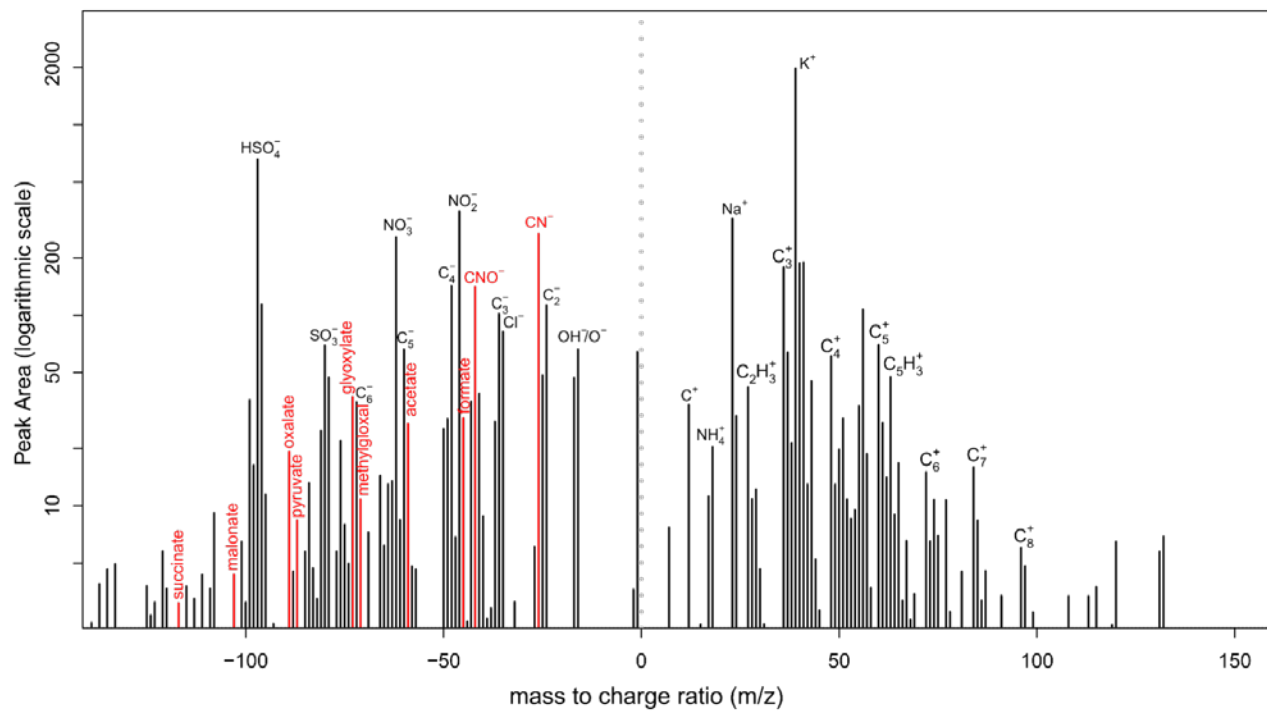
910

911   Fig. 1.
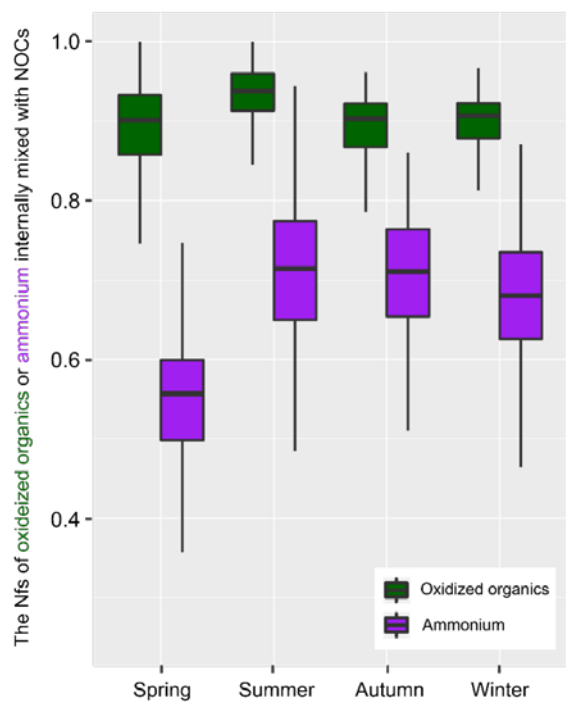
912

913   Fig. 2.
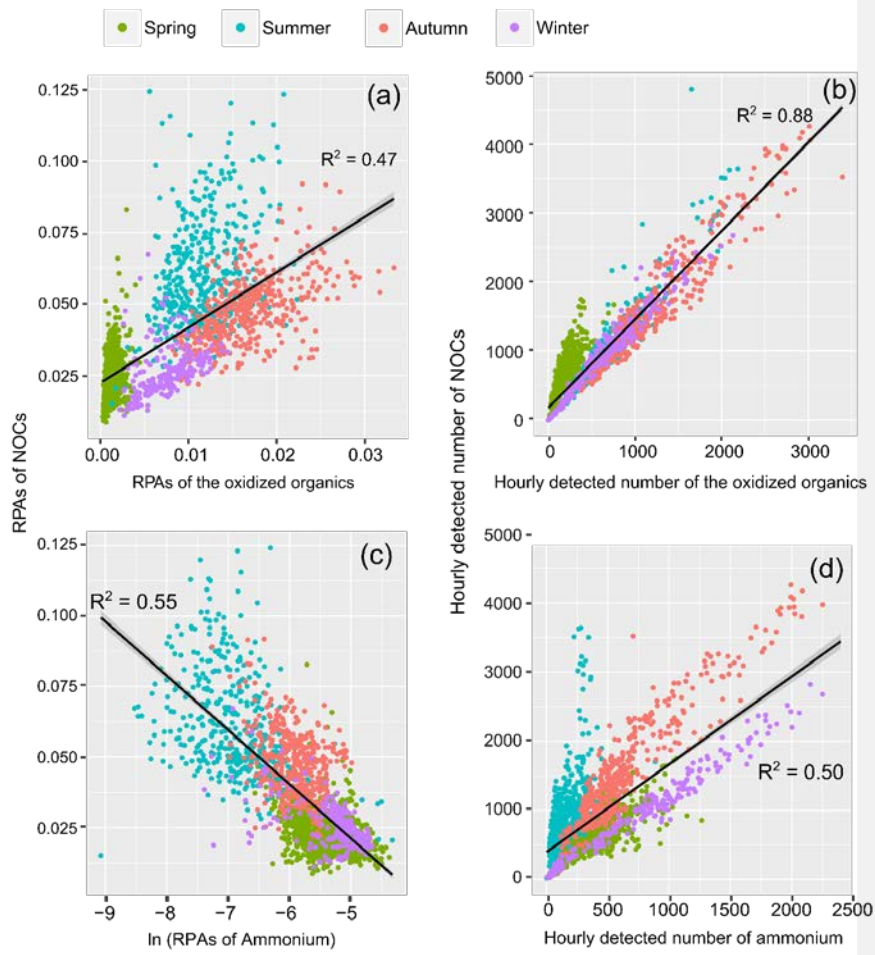
914

915   Fig. 3.
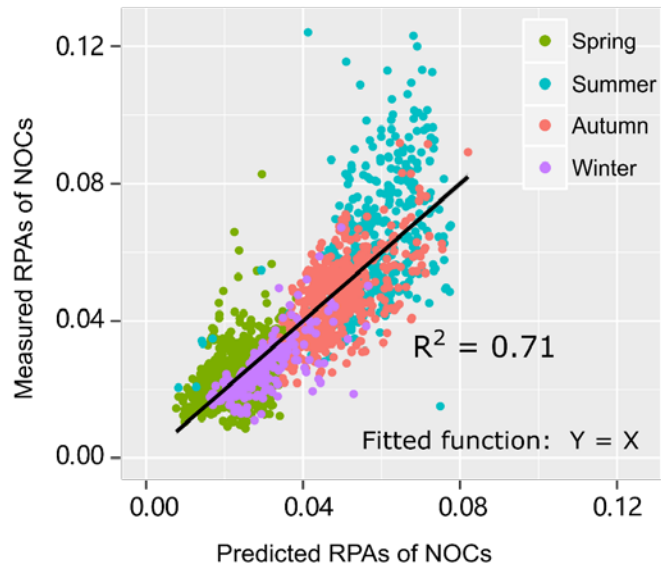
916

917   **Fig. 4.**

918

919

920   **Fig. 5.**

921
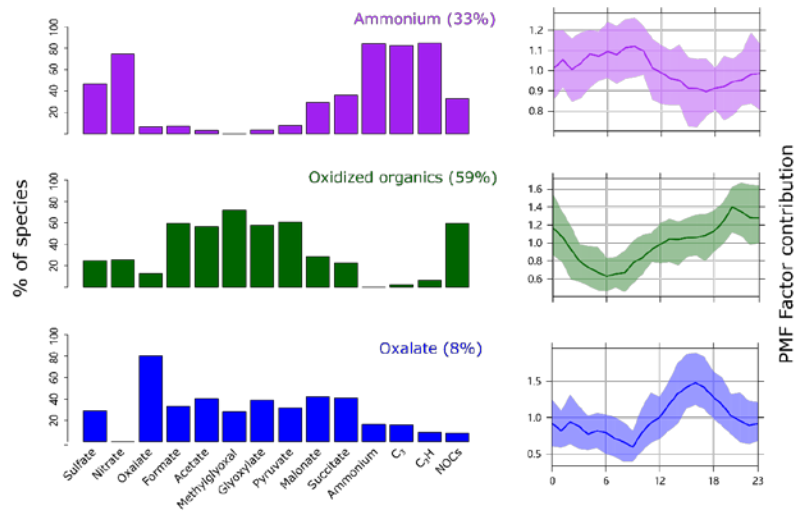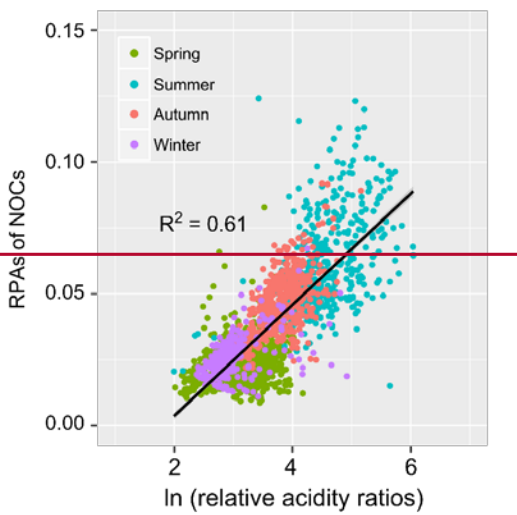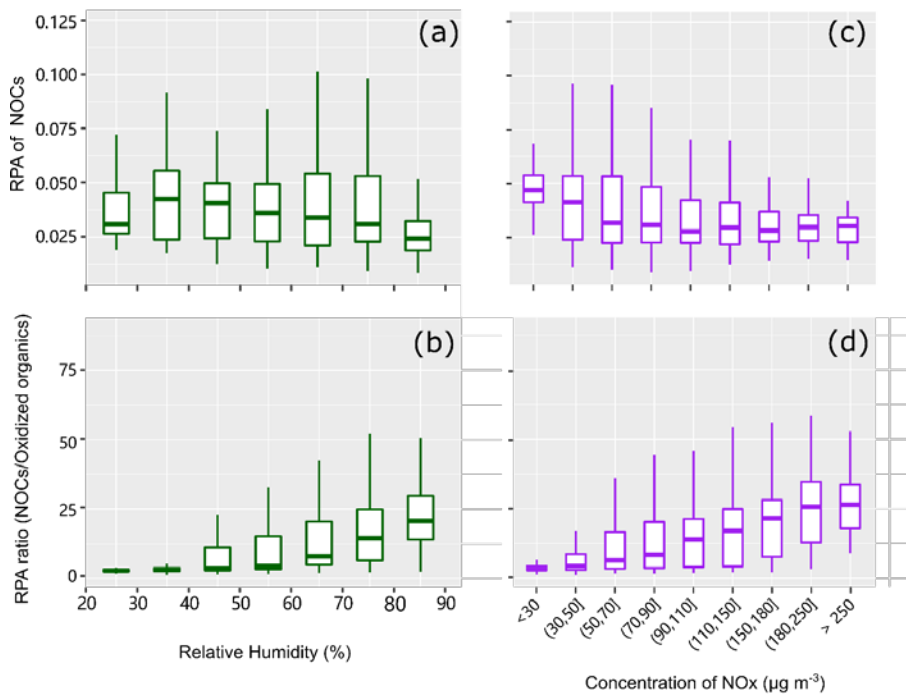
922   **Fig. 6.**   **Fig. 7.**

1 Supporting Information for

2 **High secondary formation of nitrogen-containing organics (NOCs) and its possible**

3 **link to oxidized organics and ammonium**

4

5 Guohua Zhang[1], Xiufeng Lian[1,2], Yuzhen Fu[1,2], Qinhao Lin[1], Lei Li[3], Wei Song[1], Zhanyong Wang[4],

6 Mingjin Tang[1], Duohong Chen[5], Xinhui Bi[1,*], Xinming Wang[1], Guoying Sheng[1]

7

8 [1] State Key Laboratory of Organic Geochemistry and Guangdong Key Laboratory of Environmental

9 Resources Utilization and Protection, Guangzhou Institute of Geochemistry, Chinese Academy of

10 Sciences, Guangzhou 510640, PR China

11 [2] University of Chinese Academy of Sciences, Beijing 100039, PR China

12 [3] Institute of Mass Spectrometer and Atmospheric Environment, Jinan University, Guangzhou 510632,

13 China

14 [4] School of Intelligent Systems Engineering, Sun Yat-sen University, Shenzhen 518107, PR China

15 [5] State Environmental Protection Key Laboratory of Regional Air Quality Monitoring, Guangdong

16 Environmental Monitoring Center, Guangzhou 510308, PR China

17

18   **Instrumentation**

19   Individual particles are introduced into SPAMS through a critical orifice. They are

20   focused and accelerated to specific velocities, which are determined by two continuous

21   diode Nd:YAG laser beams (532 nm). Based on the measured velocities, a pulsed laser

22   (266 nm) downstream is trigger to desorp/ionize the particles. The produced positive and

23   negative molecular fragments are recorded. In summary, a velocity, a detection moment,

24   and an ion mass spectrum are recorded for each ionized particle, while there is no mass

25   spectrum for not ionized particles. The velocity could be converted to d_{va} based on a

26   calibration using polystyrene latex spheres (PSL, Duke Scientific Corp., Palo Alto) with

27   predefined sizes. It is noted that pure ammonium sulfate is difficult to be ionized under 266

28   nm UV laser used in the SPAMS, although this may not be the case since we focused on

29   the NOCs-containing particles.

30   The concentrations of NO_x, and O_3 were measured by Model 42i (NO-NO_2-NO_x)

31   Analyzer, and Model 49i O_3 Analyzer (Thermo Fisher Scientific Inc.), respectively. The

32   concentrations of $PM_{2.5}$ were continuously measured using a tapered element oscillating

33   microbalance (TEOM 1405, Thermo Fisher Scientific Inc.), respectively.

34

35   **Positive matrix factorization**

36   PMF is a multivariate receptor model used to determine source factors, and it has

37   been used extensively with temporal variation data. In order to complement single

38   particle data analysis, we used USEPA PMF 5.0 (Norris et al., 2009) to group chemical

39   markers from all the detected particles. In such analysis, RPAs for ion markers were

40   typically used as input in the PMF model. An uncertainty of 50% in RPA was used due to

41   the shot-to-shot fluctuations of desorption laser and complex particle matrix (Zauscher et

42   al., 2013). 14 marker ions with were used, including sulfate ($-97[HSO_4]^-$), nitrate (-

43   $62[NO_3]^-$), ammonium ($18[NH_4]^+$), oxalate ($89[HC_2O_4]^-$), oxidized organics markers (at

44   m/z $-45[HCO_2]^-$, m/z $-59[CH_3CO_2]^-$, m/z $-71[C_3H_3O_2]^-$, m/z $-73[C_2HO_3]^-$, m/z -

45   $87[C_3H_3O_3]^-$, m/z $-103[C_3H_3O_4]^-$, and m/z $-117[C_4H_5O_4]^-$), organic nitrogen markers

46   (NOCs, sum of $-42[CNO]^-$ and $-26[CN]^-$), and other carbonaceous fragments (i.e.,

47   $36[C_3]^+$, $37[C_3H]^+$).

48   PMF solutions with 2−5 factors were tested and showed convergence results. The

49   relevant Q values and Q_{robust} / Q_{theory} for these solutions are shown in Table S3. In these

50   solutions explored Q_{robust} / Q_{theory} < 1, although it is recommended that $Q_{robust} \approx Q_{theory}$.

51   The 3-factor solution was chosen as the best because the measured versus predicted RPA

52   of more relevant chemical species (i.e., NOCs, the oxidized organics and ammonium) in

53   the PMF model had strong correlations ($R^2 = 0.56−0.95$), and also has the most

54   physically meaningful factors. The residuals of this solution were between -2 and 2. In

55   the 4 and 5-factor solution, with slightly stronger R^2 values than the 3-factor solution for

56   NOCs and ammonium, but had two similar oxalate factors or an additional methylglyoxal

57   factor, respectively, which seemed less physically meaningful. Bootstrapping on the 3-

58   factor solution shows stable results, with > 90 out of 100 bootstrap factors mapped with

59   those in the based run. Fpeak value from −0.5 to 0.5 was examined, and an examination

60   of Q values showed the application of Fpeak of 0 giving the best result.

61

62 **Limited dependent of NOCs on the oxidized organics during spring and ammonium**

63 **during summer**

64 During summer, the hourly detected number of NOCs showed a limited dependent on

65 ammonium (Fig. 3d). As shown in Fig. S4, the detected number of ammonium is obviously

66 lower than NOCs. In contrast, there were prevalent oxidized organics that were associated

67 with NOCs. Due to the volatility of ammonium nitrate, there is less particulate ammonium

68 in summer. Higher level of NH_3 during summer (Pan et al., 2018) may have potential

69 influence on the formation of NOCs. Less dependence of NOCs on ammonium could be

70 due to the more predominant formation of secondary NOCs through the uptake of NH_3 and

71 the following interactions with secondary oxidized organics. As shown by Nguyen et al.

72 (2012), ammonia is more efficient for the formation of NOCs in this pathway than

73 ammonium. As also supported with PMF results shown in Fig. 5, the oxidized organics

74 factor dominant contributed to the predicted NOCs during warmer seasons. Limited

75 ammonium in this factor may also indicate that abundance of oxidized organics during

76 warmer season consumed the available ammonium. As discussed, such chemistry would

77 even lead to a reduction in the concentrations of NH_3 and NH_4^+ through a model simulation

78 (Zhu et al., 2018). However, NOCs showed a limited dependent on the oxidized organics

79 during spring (Fig. 3a and 3b). Consistently, the lowest fraction of NOCs that contained

80 the oxidized organics was observed (Fig. S4), and ammonium factor explained ~80% of

81 the predicted NOCs (Fig. 5) during spring. It is likely attributed to the higher conversion

82 of oxidized organics to the observed NOCs in humid air during spring (Fig. 6 and Table

83 S1). In addition, possible reasons might also include more primary NOCs and unidentified

84 oxidized organics.

85   Table S1. The number and Nfs of NOCs-containing particles in the all the detected

86   particles during four seasons, respectively. Standard errors for the Nfs of particles were

87   estimated assuming Poisson distribution(Pratt et al., 2010). Temperature (T), relative

88   humidity (RH), O_3, and $PM_{2.5}$ were provided by Guangdong Environmental Monitoring

89   Center. The arriving air masses in Guangzhou, have been described previously: prevalence

90   of marine air masses in spring and summer, whereas northern air masses from inland China

91   in autumn and winter.

92

	Spring	Summer	Autumn	Winter
Num. of all the detected particles	933934	719371	1202604	397637
Nfs of NOCs-containing particles	58.7 ± 0.08%	59.4 ± 0.09%	59.0 ± 0.07%	55.6 ± 0.1%
Temperature (ºC)	18.8 ± 4.2	29.0 ± 2.7	24.9 ± 2.6	11.3 ± 2.3
Relative Humidity (%)	68.0 ± 13.4	66.0 ± 11.4	47.0 ± 10.1	43.0 ± 19.1
O_x (µg m^{-3})	100.4 ± 43.7	114.5 ± 70.6	136.3 ± 35.4	113.1 ± 34.0
$PM_{2.5}$ (µg m^{-3})	51.2 ± 26.0	31.9 ± 21.0	44.3 ± 18.1	55.3 ± 28.9

93

94 Table S2. Coefficients calculated with a multiple linear regression analysis of the

95 RPAs of NOCs and those of the oxidized organics and ammonium. All the regressions

96 show significant correlation, with the fitting coefficients shown with a standard error.

97

	The oxidized organics	Ln (Ammonium)	R^2
Spring	4.24 ± 0.36	-0.0064 ± 0.00057	0.24
Summer	1.69 ± 0.22	-0.012 ± 0.0013	0.24
Autumn	1.27 ± 0.09	-0.0086 ± 0.0011	0.38
Winter	1.57 ± 0.14	-0.0010 ± 0.00069	0.57
Autumn 2014	1.18 ± 0.11	-0.013 ± 0.0042	0.35

98

99   Table S3. Q values for PMF Analysis with different number of factors.

100

Num. of factors	$R^{2\#}$ for all the input species	R^2 for NOCs	R^2 for the oxidized organics	R^2 for ammonium	Q_{robust} *	Q_{robust}/Q_{theory}
2	0.28-0.95	0.28	0.44-0.95	0.46	12110	0.76
3	0.25-0.95	0.74	0.59-0.95	0.56	8278	0.59
4	0.49-0.92	0.78	0.59-0.92	0.64	6485	0.53
5	0.41-0.94	0.83	0.58-0.94	0.66	4944	0.47

101

102        $^{\#}R^2$ between the observed and predicted species

103   * Q_{robust} with $F_{peak} = 0$.

The plot shows Number Fraction (y-axis, 0.0 to 0.8) versus m/z (x-axis, 0 to 200). Labeled peaks: 17⁻, 26⁻, 42⁻, 59⁻, 80⁻, 97⁻.

104

105
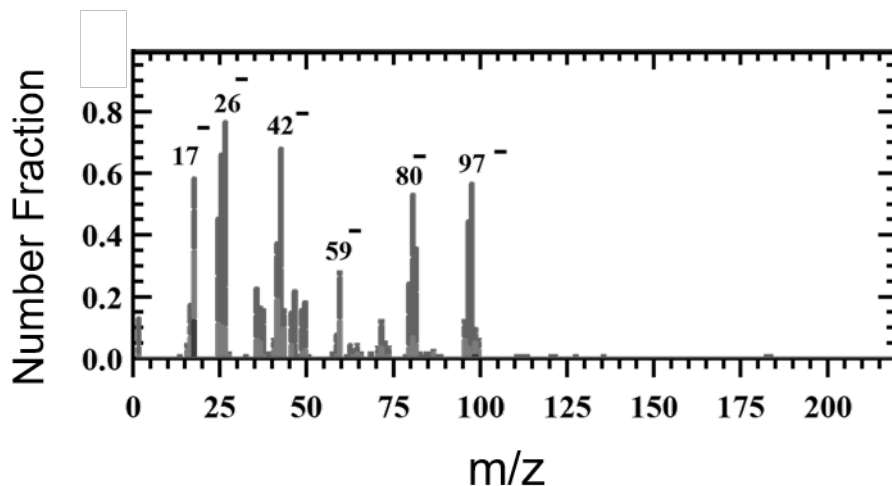
Figure S1. The number fraction of ion peaks versus m/z from the bulk solution-phase

reaction of ammonium sulfate and methylglyoxal. The bulk solution-phase reaction was

prepared with 1M ammonium sulfate and 1M methylglyoxal solution, and aged in sealed

bottles under dark conditions and at room temperature for several days. BrC SOA formed

from such reaction has been previously reported to be significantly contributed from

NOCs (Aiona et al., 2017).
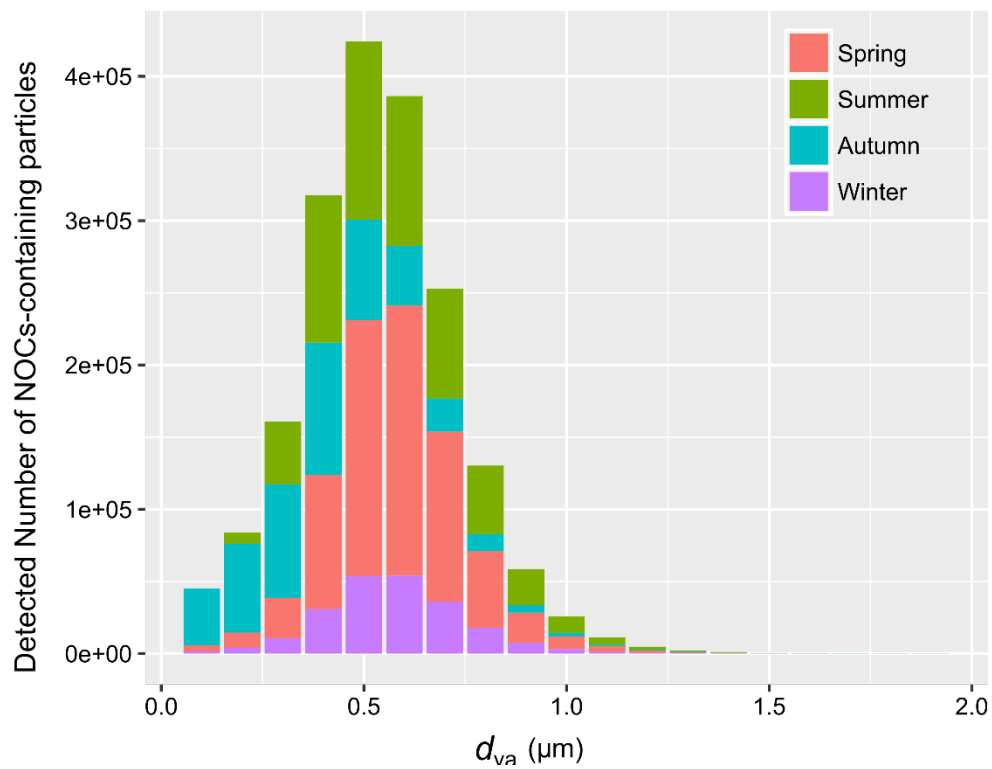
112

113

114 **Figure S2.** The detected number of NOC-containing particles along d_{va}.
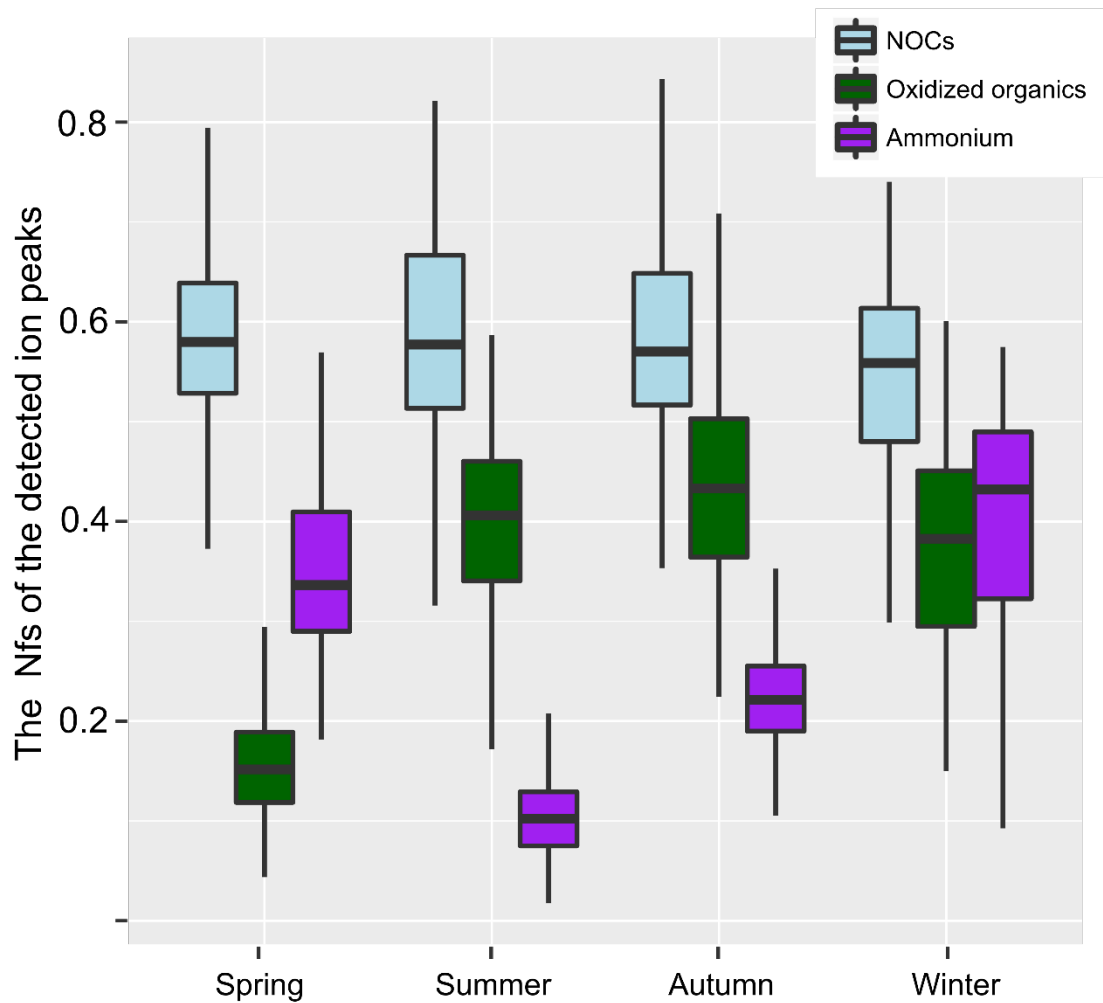
115
116

117 **Figure S3.** The distribution of the Nfs of the detected ion peaks over four seasons.

(a) Spring

(b) Summer

Ammonium   Oxidized organics   NOCs

(c) Autumn

(d) Winter
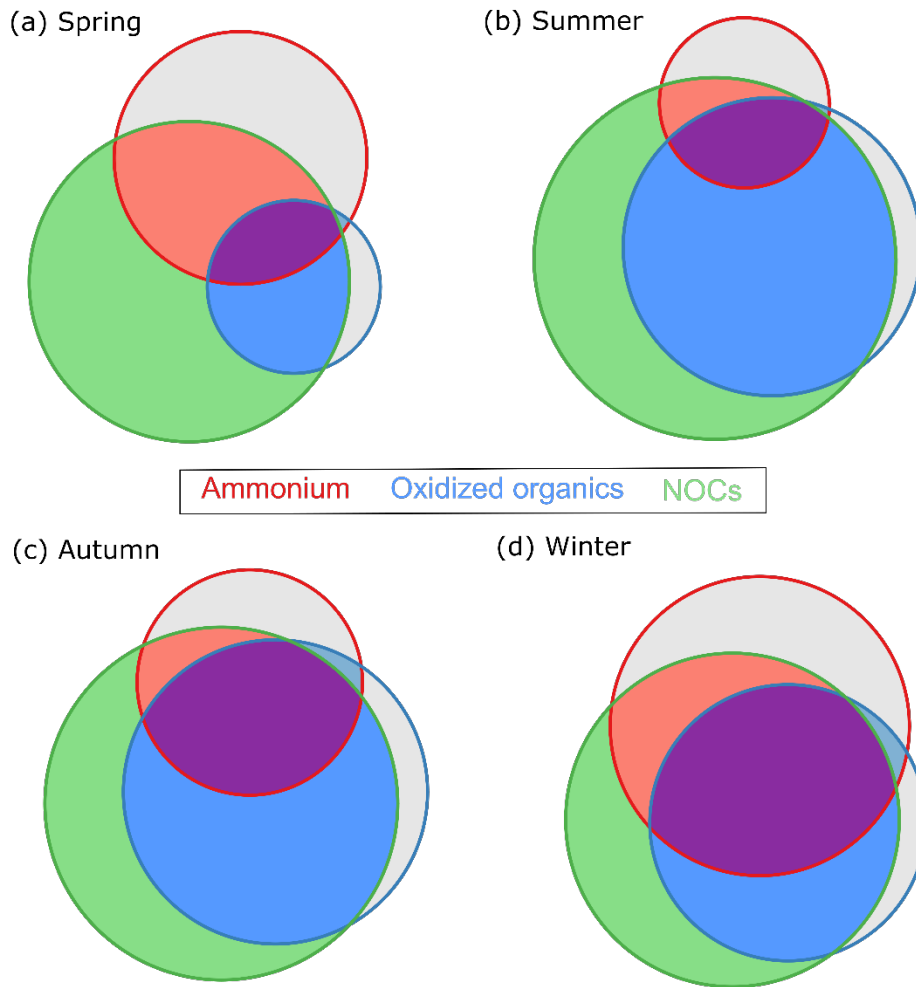
118
119

120   Figure S4. Venn plot of number based mixing state involving NOCs (green circle), the

121   oxidized organics (blue circle), and ammonium (red circle).
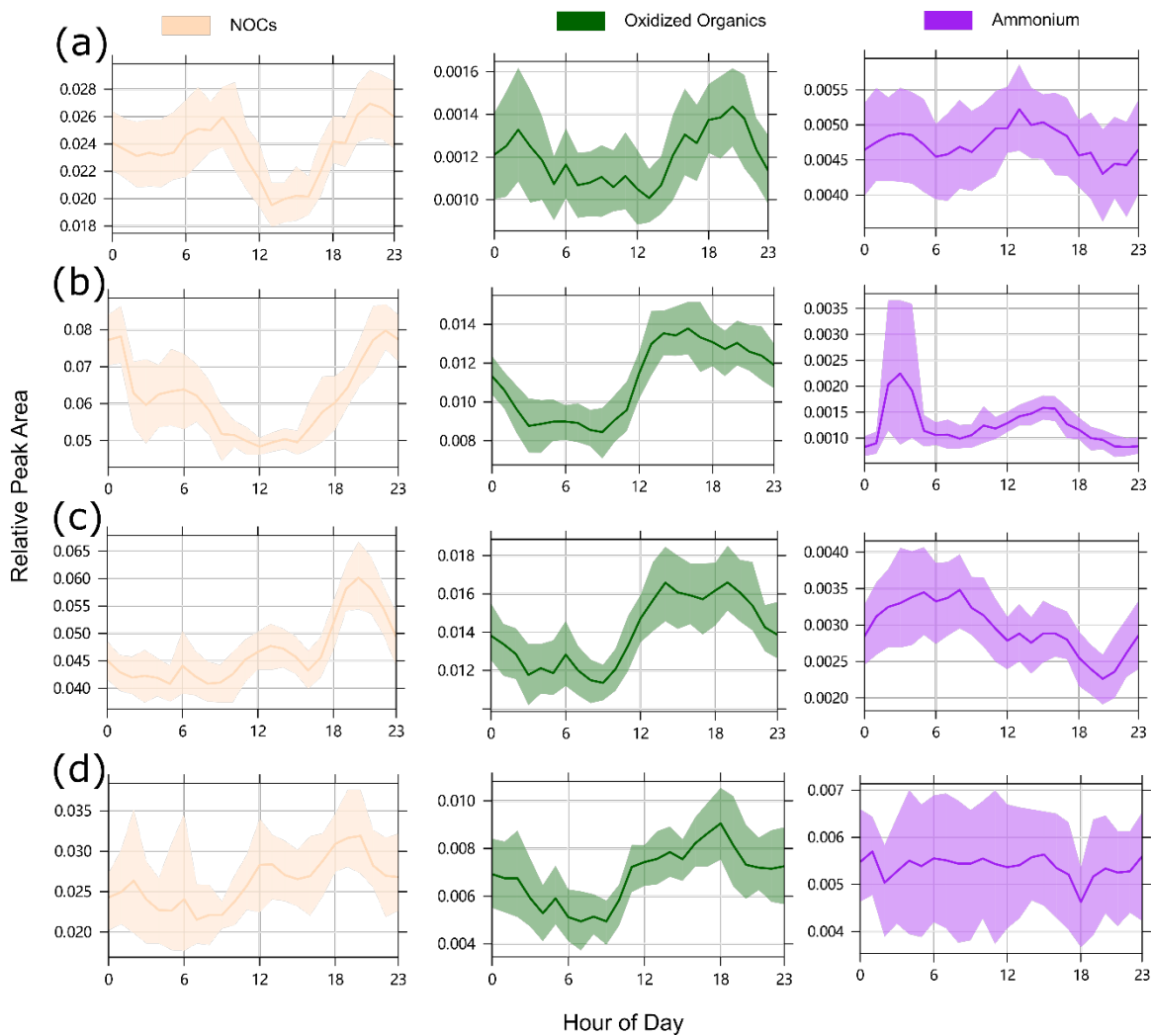
Figure S5. Diurnal variations of RPAs of NOCs, oxidized organics, and ammonium from spring to winter (a-d).

Y = −1.07*X + 2

R^2=0.58

In (NH_4)
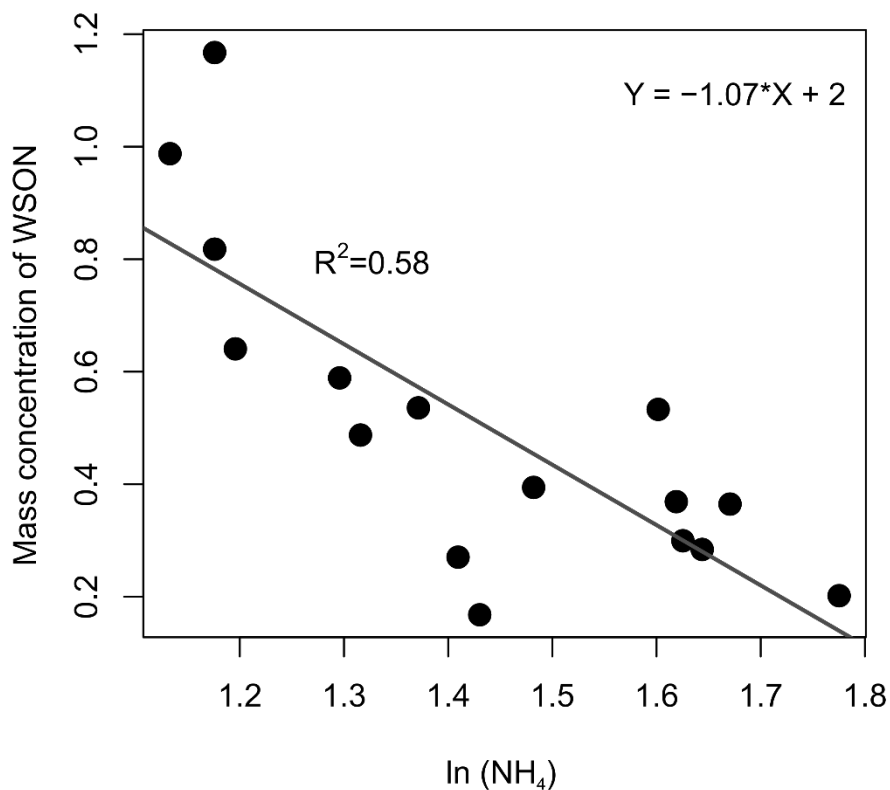
126
127

128 Figure S6. Relationship between the mass concentration of WSON and ammonium

129 (logarithmic transformed) in submicron particles during autumn of 2014. It is noted that

130 WSON (represented as the mass concentration of organic N) might not be properly

131 regarded as NOCs, as no significant correlation between daily mean mass

132 concentrations/fraction of WSON and the RPAs of NOCs. This is probably because the

133 daily mean values calculated for the RPAs of NOCs miss the temporal variation

134 information. Also, a part of NOCs might not be water-soluble (Cape et al., 2011).

135   During the autumn of 2014, daily size-resolved quartz fiber filter samples were

136 collected using an Andersen PM_{10} sampler equipped with a size-selective inlet high

137 volume cascade impactor (Model SA235, Andersen Instruments Inc.). The filters were

138 baked for 4 h in a muffle furnace at 500 °C before use. Water-soluble inorganic ions were

139   analyzed by ion chromatography (Metrohm 883, Switzerland). In addition, water soluble

140   organic carbon (WSOC) and nitrogen (WSON) were analyzed by a Total Organic Carbon

141   Analysis Instrument (TOC, Germany). It is noted that NOCs, the oxidized organics, and

142   ammonium during this period also showed a similar relationship with that during autumn

143   of 2013.
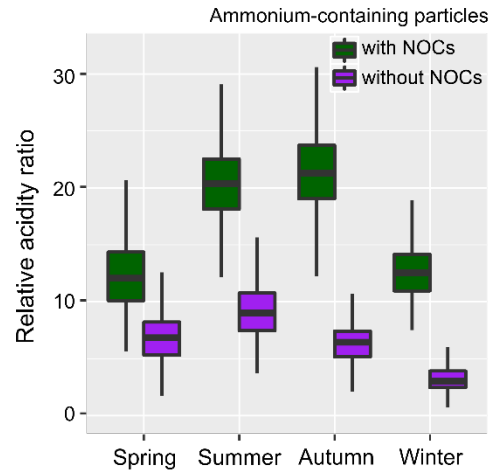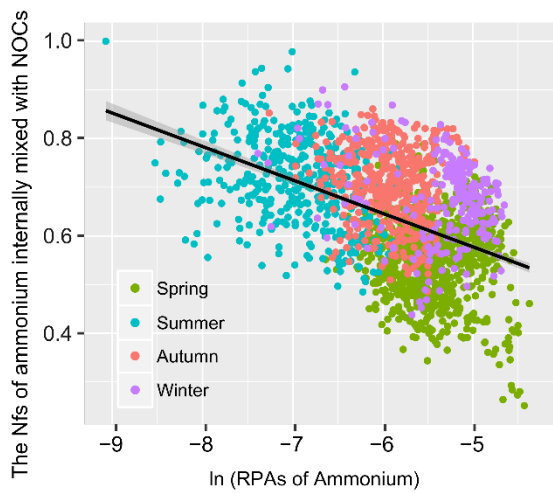
144
145

146   Figure S7. Relationship between the Nfs of ammonium that was internally mixed with

147   NOCs and RPAs of ammonium (left), and comparison of the relative acidity ratio

148   between ammonium-containing particles internally and externally mixed with NOCs

149   (right).

12
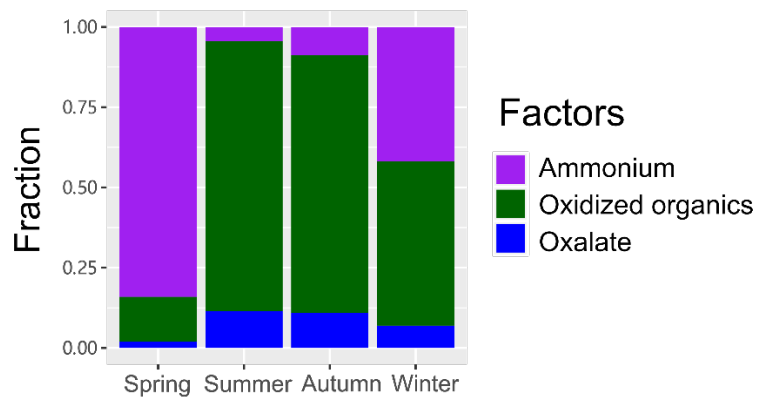
150
151

152   Figure S8. The relative contributions of the PMF-resolved 3-factor to the modelled NOCs

153   over the seasons.

154   References

155   Aiona, P. K., Lee, H. J., Leslie, R., Lin, P., Laskin, A., Laskin, J., and Nizkorodov, S. A.:

156   Photochemistry of Products of the Aqueous Reaction of Methylglyoxal with Ammonium

157   Sulfate, Acs Earth Space Chem., 1, 522-532, doi:10.1021/acsearthspacechem.7b00075,

158   2017.

159   Cape, J. N., Cornell, S. E., Jickells, T. D., and Nemitz, E.: Organic nitrogen in the atmosphere —

160   Where does it come from? A review of sources and methods, Atmos. Res., 102, 30-48,

161   doi:10.1016/j.atmosres.2011.07.009, 2011.

162   Norris, G., Vedantham, R., Wade, K., Zahn, P., Brown, S., Paatero, P., Eberly, S., and Foley, C.

163   (2009), Guidance document for PMF applications with the Multilinear Engine, edited,

164   Prepared for the U.S. Environmental Protection Agency, Research Triangle Park, NC.

165   Pratt, K. A., Heymsfield, A. J., Twohy, C. H., Murphy, S. M., DeMott, P. J., Hudson, J. G.,

166   Subramanian, R., Wang, Z. E., Seinfeld, J. H., and Prather, K. A.: In Situ Chemical

167   Characterization of Aged Biomass-Burning Aerosols Impacting Cold Wave Clouds, J.

168   Atmos. Sci., 67, 2451-2468, doi:10.1175/2010JAS3330.1, 2010.

169   Zauscher, M. D., Wang, Y., Moore, M. J. K., Gaston, C. J., and Prather, K. A.: Air Quality Impact

170   and Physicochemical Aging of Biomass Burning Aerosols during the 2007 San Diego

171   Wildfires, Environ. Sci. Technol., 47, 7633-7643, doi:10.1021/es4004137, 2013.

172   Zhu, S. P., Horne, J. R., Montoya-Aguilera, J., Hinks, M. L., Nizkorodov, S. A., and Dabdub, D.:

173   Modeling reactive ammonia uptake by secondary organic aerosol in CMAQ: application to

174   the continental US, Atmos. Chem. Phys., 18, 3641-3657, doi:10.5194/acp-18-3641-2018,

175   2018.